Synthesis and Structures of Cationic Aluminum and Gallium Amidinate Complexes

Samuel Dagorne,[†] Ilia A. Guzei,[‡] Martyn P. Coles,[†] and Richard F. Jordan*,[†]

Contribution from the Departments of Chemistry, The University of Iowa, Iowa City, Iowa, 52242, and Iowa State University, Ames, Iowa, 50011

Received June 21, 1999

Abstract: Aluminum and gallium amidinate complexes, $\{RC(NR')_2\}MMe_2$ (R, R' = alkyl; M = Al, Ga), react with the "cationic activators" $[Ph_3C][B(C_6F_5)_4]$ and $B(C_6F_5)_3$ to yield cationic Al and Ga alkyl species whose structures are strongly influenced by the steric properties of the amidinate ligand. The reaction of acetamidinate Al complexes $\{MeC(NR')_2\}AlMe_2$ (R' = ^iPr, **1a**; R' = Cy, **3a**) with 0.5 equiv of $[Ph_3C][B(C_6F_5)_4]$ or $B(C_6F_5)_3$ yields $\{MeC(NR')_2\}_2Al_2Me_3^+$ (R' = ^iPr, **2a**$^+$; R' = Cy, **4a**$^+$) as the $B(C_6F_5)_4^-$ or $MeB(C_6F_5)_3^-$ salts. X-ray crystallographic analyses establish that **2a**$^+$ and **4a**$^+$ are double-amidinate-bridged dinuclear cations, in which the two metal centers are linked by μ-η^1,η^1 and μ-η^1,η^2 amidinate bridges. NMR studies show that **2a**$^+$ undergoes two dynamic processes in solution: (i) a μ-$\eta^1,\eta^1/\mu$-η^1,η^2 amidinate exchange and (ii) Me exchange between the two metal centers. The reaction of $\{MeC(N^iPr)_2\}GaMe_2$ (**1b**) with 0.5 equiv of $B(C_6F_5)_3$ yields $\{MeC(N^iPr)_2\}_2Ga_2Me_3^+$ (**2b**$^+$), whose structure and dynamic properties are similar to those of **2a**$^+$. The reaction of the bulkier ^tBu-substituted amidinate complexes $\{^tBuC(N^iPr)_2\}MMe_2$ (M = Al, **6a**; M = Ga, **6b**) with 0.5 equiv of $[Ph_3C][B(C_6F_5)_4]$ yields $\{^tBuC(N^iPr)_2\}MMe_2\cdot\{^tBuC(N^iPr)_2\}MMe^+$ (M = Al, **7a**$^+$; M = Ga, **7b**$^+$) as the $B(C_6F_5)_4^-$ salts, the former of which is thermally unstable. An X-ray crystallographic analysis establishes that **7b**$^+$ is a single-amidinate-bridged dinuclear cation, in which the two metal centers are linked by a μ-η^1,η^2 amidinate bridge. NMR data establish that the structures of **7a**$^+$ and **7b**$^+$ are similar and both species are rigid in solution. **6a** and **6b** also react with $B(C_6F_5)_3$ to yield $[\textbf{7a}][MeB(C_6F_5)_3]$ and $[\textbf{7b}][MeB(C_6F_5)_3]$, respectively, which decompose by $C_6F_5^-$ transfer to yield $\{^tBuC(N^iPr)_2\}M(Me)(C_6F_5)$ (M = Al, **9a**; M = Ga, **9b**) and boron species. The "super-bulky" amidinate complexes $\{^tBuC(N^tBu)_2\}MMe_2$ (M = Al, **12a**; M = Ga, **12b**) react with 1 equiv of $[Ph_3C][B(C_6F_5)_4]$ to yield $\{^tBuC(N^tBu)_2\}MMe^+$ (M = Al, **13a**$^+$; M = Ga, **13b**$^+$) as the $B(C_6F_5)_4^-$ salts. The salts $[\textbf{13a}][B(C_6F_5)_4]$ and $[\textbf{13b}][B(C_6F_5)_4]$ are thermally unstable and could not be isolated. However, the NMR data for **13a**$^+$ and **13b**$^+$ in C_6D_5Cl are consistent with base-free, three-coordinate structures or labile, four-coordinate solvated cations. These results provide a starting point for understanding the mechanism and reactivity trends in ethylene polymerization catalyzed by cationic Al amidinate species.

Introduction

Neutral aluminum complexes, $(AlX_3)_2$ (X = halide, alkyl, alkoxide, etc.), are widely used as reagents or catalysts for Lewis acid-mediated reactions (Friedel−Crafts, Diels−Alder, etc.), alkylating agents, initiators for cationic polymerizations, and cocatalysts/activators in transition-metal-catalyzed olefin polymerizations.[1] Additionally, neutral Al alkyls catalyze the oligomerization of ethylene to α-olefins at elevated temperatures and ethylene pressures.[2] *Cationic* aluminum complexes are of potential interest for many of these applications because of the possibility that the increased electrophilicity resulting from the cationic charge may enhance substrate coordination and activa-

tion.[3] Recent developments in this area include (i) cationic polymerization of isobutylene and isobutylene/isoprene by Cp_2-Al^+,[3a] (ii) ring-opening polymerization of propylene oxide by $(salen)Al(MeOH)_2^+$, $(acen)Al(MeOH)_2^+$,[3b] $\{\eta^3$-MeN$((CH_2)_2$-$NMe_2)_2\}AlMe_2^+$, and $\{\eta^3$-HRN$(CH_2)_2NR'(CH_2)_2NR\}AlCl^+$,[3c,d] (iii) ring-opening polymerization of D,L-lactide by $\{HRN(CH_2)_2$-$NR'(CH_2)_2NR\}AlCl^+$,[3d] and (iv) catalysis of enantioselective Diels−Alder reactions by chiral cationic boron species.[3e] Additionally, cationic Al alkyls have been reported to polymerize ethylene, but the active species in these reactions have not yet been identified.[4]

---

* Address correspondence to this author at The Department of Chemistry, The University of Chicago, 5735 S. Ellis Ave., Chicago, IL 60637.
    [†] The University of Iowa.
   [‡] Iowa State University.
    (1) (a) Starowieyski, K. B. In *Chemistry of Aluminium, Gallium, Indium and Thallium*, Downs, A. J., Ed.; Chapman & Hall: London, UK, 1993; pp 322−371. (b) Eisch, J. J. In *Comprehensive Organometallic Chemistry II*; Abel, E. W., Stone, F. G. A., Wilkinson, G., Eds.; Elsevier: Oxford, UK, 1995; Vol. 11, Chapter 6. (c) Matyjaszewski, K., Ed. *Cationic Polymerizations: Mechanisms, Synthesis and Applications*; Marcel Dekker: New York, 1996. (d) Kennedy, J. P.; Marechal, E. *Carbocationic Polymerization*; Wiley-Interscience: New York, 1982. (e) Eisch, J. J. In *Comprehensive Organometallic Chemistry II*; Abel, E. W., Stone, F. G. A., Wilkinson, G., Eds.; Elsevier: Oxford, UK, 1995; Vol. 1, Chapter 10.

(2) (a) Ziegler, K., Gellert, H. G. *Justus Liebigs Ann. Chem.* **1950**, *567*, 195. (b) Skinner, W. A.; Bishop, E.; Cambour, P.; Fuqua, S.; Lim, P. *Ind. Eng. Chem.* **1960**, *52*, 695. (c) Skupínska, J. *Chem. Rev.* **1991**, *91*, 613. (d) Al-Jarallah, A. M.; Anabtawi, J. A.; Siddiqui, M. A. B.; Aitani, A. M.; Al-Sa'doun, A. W. *Catal. Today* **1992**, *14*, 42.

(3) (a) Bochmann, M.; Dawson, D. M. *Angew. Chem., Int. Ed. Engl.* **1996**, *35*, 2226. (b) Atwood, D. A.; Jegier, J. A.; Rutherford, D. *J. Am. Chem. Soc.* **1995**, *117*, 6779. (c) Jegier, J. A.; Atwood, D. A. *Inorg. Chem.* **1997**, *36*, 2034. (d) Emig, N.; Nguyen, H.; Krautscheid, H.; Reau, R.; Cazaux, J. B.; Bertrand, G. *Organometallics* **1998**, *17*, 3599. (e) Hayashi, Y.; Rohde, J. J.; Corey, E. J. *J. Am. Chem. Soc.* **1996**, *118*, 5502. (f) For a review, see: Atwood, D. A. *Coord. Chem. Rev.* **1998**, *176*, 407.

(4) (a) Coles, M. P.; Jordan, R. F. *J. Am. Chem. Soc.* **1997**, *119*, 8125. (b) Ihara, E.; Young, V. G., Jr.; Jordan, R. F. *J. Am. Chem. Soc.* **1998**, *120*, 8277. (c) Bruce, M.; Gibson, V. C.; Redshaw, C.; Solan, G. A.; White, A. J. P.; Williams, D. J. *Chem. Commun.* **1998**, 2523.

Chart 1

R, R' = hydrocarbyl

L = Lewis Base
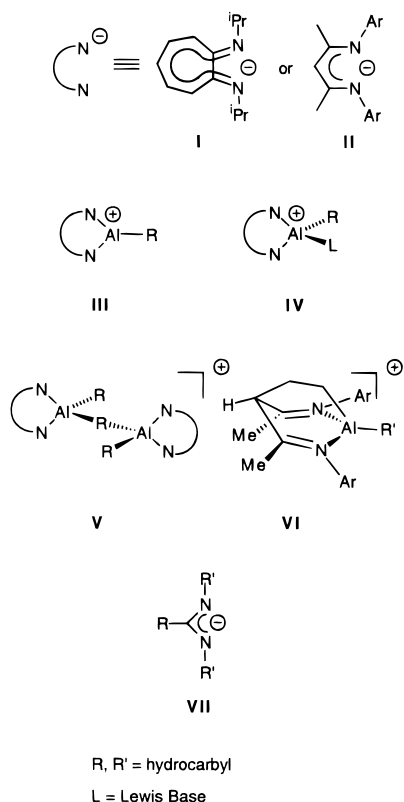
Three-coordinate cationic Al alkyls of general type {L−X}-AlR$^+$ that are stabilized by monoanionic bidentate L−X$^-$ ligands are attractive targets for investigation because they represent a reasonable balance of electrophilicity and stability. The use of bidentate stabilizing ligands may alleviate complications from ligand redistribution reactions, a common feature in Al chemistry.[1a] In contrast, simple two-coordinate AlR$_2^+$ species (R = Me, Et) appear to react rapidly with B(C$_6$F$_5$)$_4^-$,[5] one of the most robust "noncoordinating" anions known,[6] while four-coordinate AlR$_2$(NR$_3$)$_2^+$ and related AlR$_2$L$_2^+$ species may need to undergo ligand dissociation prior to substrate binding in many cases. We have described the synthesis and reactivity of {L−X}AlR$^+$ species containing *N,N*-diisopropylaminotroponiminate (ATI, **I**, Chart 1) and *N,N*-diaryldiketiminate ligands (**II**) which form five- and six-membered chelate rings with Al.[4b,7] Neutral {L−X}AlR$_2$ complexes based on **I** and **II** react readily with the "cationic activators" [Ph$_3$C][B(C$_6$F$_5$)$_4$], B(C$_6$F$_5$)$_3$ and [NHMe$_2$-Ph][B(C$_6$F$_5$)$_4$] to yield cationic products whose structures are strongly influenced by the steric properties of the L−X$^-$ ligand and the nature of the Al−R alkyl group. Thus far, three structural types have been characterized: base-free three-coordinate species **III**, base-stabilized four-coordinate cations **IV**, and dinuclear Me-bridged cations **V**. Base-free (ATI)AlR$^+$ (R = Et, ^{i}Bu) species polymerize ethylene,[4b,8] while base-free {diketiminate}AlR$^+$ species undergo an unusual cycloaddition reaction with ethylene and other unsaturated hydrocarbons to give bicyclic complexes of type **VI**.[7]

Amidinate ligands, RC(NR′)$_2^-$ (**VII**), are interesting candidates for application as ancillary ligands in {L−X}AlR$^+$ species because their steric and metal-binding properties can be modified by variation of the amidinate substituents, and they form compact four-membered {RC(NR′)$_2$}Al chelate rings resulting in sterically open Al centers.[9] We recently reported that {RC-(NR′)$_2$}AlMe$_2$ complexes react with cationic activators to yield cationic Al species which polymerize ethylene.[4a,10] Here we describe the structures and dynamic properties of the cationic Al species formed in these systems. As will be seen, the chemistry of cationic Al amidinate species is more complicated than that of cationic complexes based on **I** and **II** due to the ability of amidinate ligands to adopt several types of chelating and bridging bonding modes. The synthesis and structures of cationic gallium species derived by methyl abstraction from {RC(NR′)$_2$}GaMe$_2$ complexes are also described. The Ga cations are considerably less reactive than the Al analogues, due to the lower polarity of the Ga−Me bonds vs the Al−Me bonds, and thus serve as useful models for the Al systems.[11] Moreover, cationic Ga alkyls are of interest for synthetic and catalytic applications involving polar substrates because of the relative stability of Ga−R bonds (vs Al−R) toward hydrolysis and electrophilic cleavage.[12]

Results

Reaction of {MeC(NR′)$_2$}AlMe$_2$ (1a, R′ = ^{i}Pr; 3a, R′ = Cy) with B(C$_6$F$_5$)$_3$ or [Ph$_3$C][B(C$_6$F$_5$)$_4$]. The reaction of **1a** with 0.5 equiv of B(C$_6$F$_5$)$_3$ or [Ph$_3$C][B(C$_6$F$_5$)$_4$] in C$_6$D$_5$Cl (10 min, 23 °C) yields the dinuclear cationic complex {MeC(N^i-Pr)$_2$}$_2$Al$_2$Me$_3^+$ (**2a$^+$**) as the MeB(C$_6$F$_5$)$_3^-$ or B(C$_6$F$_5$)$_4^-$ salt, respectively (100% by ^{1}H NMR vs an internal standard, Scheme 1). For [**2a**][B(C$_6$F$_5$)$_4$], the presence of 1 equiv of Ph$_3$CMe (vs **2a$^+$**) was also observed by ^{1}H NMR. [**2a**][MeB(C$_6$F$_5$)$_3$] and [**2a**]-[B(C$_6$F$_5$)$_4$] do not react further with excess B(C$_6$F$_5$)$_3$ or [Ph$_3$C]-[B(C$_6$F$_5$)$_4$] at 23 °C as shown by ^{1}H and ^{19}F NMR. [**2a**][MeB-(C$_6$F$_5$)$_3$] slowly decomposes in CD$_2$Cl$_2$ ($t_{1/2} \approx 5$ h, 23 °C) and C$_6$D$_5$Cl ($t_{1/2} \approx 18$ h, 23 °C) to unidentified species, whereas [**2a**][B(C$_6$F$_5$)$_4$] is stable in those solvents at 23 °C for several days. [**2a**][MeB(C$_6$F$_5$)$_3$] and [**2a**][B(C$_6$F$_5$)$_4$] were isolated as analytically pure colorless solids in 83% and 78% yield, respectively, by generation in CH$_2$Cl$_2$, removal of volatiles, and pentane washing.[13] Initial NMR studies suggested that **2a$^+$** adopts a Me-bridged structure.[4a] However, more extensive NMR and crystallographic results establish that **2a$^+$** adopts an amidinate-bridged structure (vide infra).

Similarly, the reaction of **3a** with 0.5 equiv of [Ph$_3$C]-[B(C$_6$F$_5$)$_4$] in hexane (3 d, 23 °C) quantitatively yields [{MeC-(NCy)$_2$}$_2$Al$_2$Me$_3$][B(C$_6$F$_5$)$_4$] ([**4a**][B(C$_6$F$_5$)$_4$]), which is isolated as an analytically pure solid by filtration (61%, Scheme 1). The ^{1}H NMR spectrum of [**4a**][B(C$_6$F$_5$)$_4$] (CD$_2$Cl$_2$) is very similar to that of [**2a**][B(C$_6$F$_5$)$_4$], except for the *Cy* resonances. [**4a**]-[B(C$_6$F$_5$)$_4$] was obtained as colorless crystals by crystallization from a mixed solvent system (10/10/1/1 hexane/pentane/C$_6$D$_5$-Cl/ClCD$_2$CD$_2$Cl, see Experimental Section).

(5) Bochmann, M.; Sarsfield, M. J. *Organometallics* **1998**, *17*, 5908.

(6) (a) Strauss, S. H. *Chem. Rev.* **1993**, *93*, 927. (b) Bochmann, M. *J. Chem. Soc., Dalton Trans.* **1996**, 255. (c) Turner, H. W. Eur. Pat. Appl. 0 277 004, 1988.

(7) (a) Radzewich, C. E.; Coles, M. P.; Jordan, R. F. *J. Am. Chem. Soc.* **1998**, *120*, 9384. (b) Radzewich, C. E.; Guzei, I. A.; Jordan, R. F. *J. Am. Chem. Soc.* **1999**, *121*, 8673. (c) Radzewich, C. E.; Jordan, R. F. Manuscript in preparation.

(8) [(ATI)AlEt][B(C$_6$F$_5$)$_4$] (toluene, 100 °C, 6 atm ethylene); activity = 1375 g PE/(mol·h·atm).

(9) (a) Edelmann, F. T. *Coord. Chem. Rev.* **1994**, *137*, 403. (b) Barker, J.; Kilner, M. *Coord. Chem. Rev.* **1994**, *133*, 219.

(10) Representative result: {^{i}BuC(N^{i}Pr)$_2$}AlMe$_2$/[Ph$_3$C][B(C$_6$F$_5$)$_4$] (toluene, 100 °C, 6 atm ethylene); activity = 2708 g PE/(mol·h·atm).

(11) χ_{Al} = 1.6 and χ_{Ga} = 1.8.

(12) Several cationic Ga methyl complexes are stable in H$_2$O, which is ascribed to the high stability of the GaMe$_2^+$ fragment. (a) Shriver, D. F.; Parry, R. W. *Inorg. Chem.* **1962**, *1*, 835. (b) Tobias, R. S.; Sprague, M. J.; Glass, G. E. *Inorg. Chem.* **1968**, *7*, 1714. (c) Olapinsky, H.; Weidlein, J. *J. Organomet. Chem.* **1973**, *54*, 87.

(13) Compound [**2a**][B(C$_6$F$_5$)$_4$] was synthesized by slow addition of **1a** to a solution of [Ph$_3$C][B(C$_6$F$_5$)$_4$] and by addition of [Ph$_3$C][B(C$_6$F$_5$)$_4$] to a solution of **1a**. Both procedures afforded [**2a**][B(C$_6$F$_5$)$_4$] in ca. 78% yield.
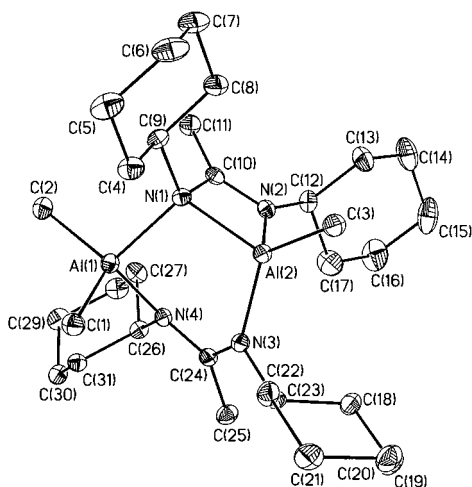
Figure 1. Molecular structure of the {MeC(NCy)$_2$}$_2$Al$_2$Me$_3^+$ cation (**4a**$^+$) in [**4a**][B(C$_6$F$_5$)$_4$]. Hydrogen atoms are omitted.

Scheme 1
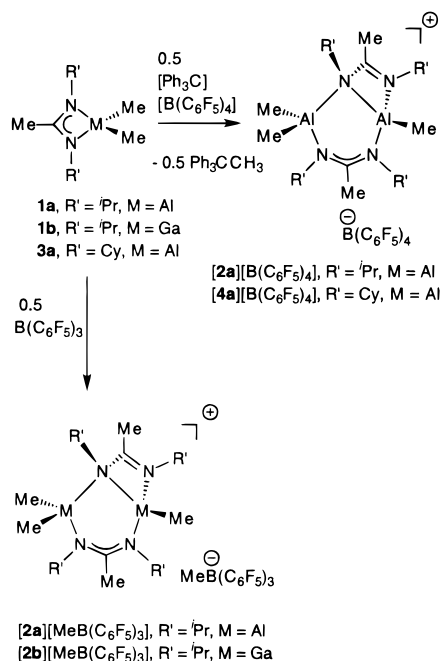
Molecular Structure of [4a][B(C$_6$F$_5$)$_4$]. [**4a**][B(C$_6$F$_5$)$_4$] crystallizes as discrete **4a**$^+$ and B(C$_6$F$_5$)$_4^-$ ions with no close cation−anion contacts. The structure of the B(C$_6$F$_5$)$_4^-$ anion is normal. The **4a**$^+$ cation (Figure 1) is a dinuclear species with C_1 symmetry. The two Al centers are linked by two different amidinate bridges: a μ-η^1,η^2 amidinate (N(1)−C(10)−N(2)), which is bonded to Al(1) through the bridging nitrogen N(1) and to Al(2) by both N(1) and N(2), and a μ-η^1,η^1 amidinate (N(3)−C(24)−N(4)), in which the two nitrogens are bonded to different Al centers. Due to their different bonding modes, the μ-η^1,η^2 and μ-η^1,η^1 amidinate units exhibit significant differences in bond distances and angles.

The C−N bond distances in the μ-η^1,η^2 amidinate are significantly different. The N(1)−C(10) distance (1.435(2) Å) is slightly shorter than the normal N−C$_{sp^2}$ single bond distance (1.47 Å),[14] and the N(2)−C(10) distance (1.289(2) Å) is comparable to the normal N−C$_{sp^2}$ double bond distance (1.27−

(14) Sutton, L. E. *Interatomic Distances and Configuration in Molecules and Ions*; Special Publications No. 18; The Chemical Society: London, 1965.

Chart 2
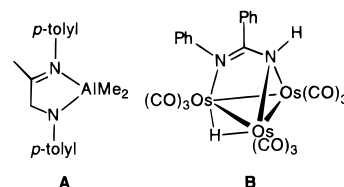
(6) Å).[15] Thus, there is little π-delocalization within the N(1)−C(10)−N(2) unit, and N(1) acts as a μ-amide donor and N(2) acts as an imine donor. The Al(2)−N(1) (1.979(1) Å) and Al(1)−N(1) (2.027(1) Å) distances are slightly longer than the Al−N bond distances in the μ-amido complex (Me$_2$Al(μ-NHAd))$_2$ (Ad = adamantyl, 1.97(2) Å average).[16] The Al(2)−N(2) distance (1.927(1) Å) is similar to those in neutral chelated amidinate complexes (e.g., **3a**, 1.92(2) Å average)[17] but is slightly shorter than the Al−N$_{imine}$ bond distance observed in neutral Al imine complexes (e.g., dimethyl{*N*-(*p*-tolyl)-2-(*p*-tolylimino)propylamino-*N,N*′}aluminum, 1.979(6) Å, **A**, Chart 2).[18] The N(1)−C(10)−N(2) angle (109.6(1)°) is typical for a chelated acetamidinate Al species (e.g., **3a**, 110.4(2)°).[17] The μ-η^1,η^2 bridge in **4a**$^+$ represents a new amidinate bonding mode. However, several examples of cluster compounds that contain triply bridging μ-η^1,η^1,η^1 amidinates are known, including Os$_3$-(μ-H)(CO)$_9${PhNC(Ph)NH} (**B**, Chart 2) and Os$_3$(μ-H)(CO)$_9$-{HNC(Me)NH}.[19]

In contrast, the N(3)−C(24) and N(4)−C(24) distances (1.360(2), 1.332(2) Å) within the μ-η^1,η^1 amidinate are intermediate between the N−C$_{sp^2}$ single and double bond distances, indicating that there is significant π-delocalization within the N(4)−C(24)−N(3) unit. The Al(1)−N(4) distance (1.959(1) Å) and the N(4)−C(24)−N(3) angle (119.0(1)°) are similar to the values in the dimeric μ-η^1,η^1 amidinate complex ({MeC-(NMe)$_2$}AlMe$_2$)$_2$ (1.92(5) Å and 118.5(1)°).[20] The Al(2)−N(3) bond distance (1.866(1) Å) is ca. 0.1 Å shorter than the Al-(2)−N(4) bond distance.

The Al centers in **4a**$^+$ adopt distorted tetrahedral geometries. The acute N(1)−Al(2)−N(2) bite angle (69.51(6)°) is normal for chelated Al amidinate complexes (e.g., **3a**, 69.96(8)°)[17] and is compensated for by the opening of the N(1)−Al(2)−C(3) (119.52(7)°) and N(2)−Al(2)−C(3) (114.32(7)°) angles. The N(2)−Al(2)−N(3) (108.64(6)°) and N(1)−Al(2)−N(3) (109.30-(6)°) angles are close to the ideal tetrahedral angle of 109.47°. The bond angles at Al(1) are closer to the ideal tetrahedral value than those at Al(2) because Al(1) has only η^1-bonded ligands. The Al−C bond distances (1.954(2) Å average) are similar to those in **3a** (1.95(7) Å average).[17]

Molecular Structure of [2a][B(C$_6$F$_5$)$_4$]. [**2a**][B(C$_6$F$_5$)$_4$] was obtained as colorless crystals by crystallization from a mixed solvent system (10/1 hexane/toluene, see Experimental Section). The X-ray structural analysis for [**2a**][B(C$_6$F$_5$)$_4$] was imprecise due to poor crystal quality but allowed determination of the connectivity and approximate metrical parameters. [**2a**][B(C$_6$F$_5$)$_4$] crystallizes as discrete **2a**$^+$ and B(C$_6$F$_5$)$_4^-$ ions, with no close

(15) Levine, I. R. *J. Chem. Phys.* **1963**, *38*, 2326.

(16) Waggoner, K. M.; Power, P. P. *J. Am. Chem. Soc.* **1991**, *113*, 3385.

(17) Coles, M. P.; Swenson, D. C.; Jordan, R. F. *Organometallics* **1997**, *16*, 5184.

(18) Kanters, J. A.; Van Mier, G. P. M.; Nijs, R. L. L. M.; Van Der Steen, F.; Van Koten, G. *Acta Crystallogr. C* **1988**, *44*, 1391.

(19) (a) Burgess, K.; Holden, D. H.; Johnson, B. F. G.; Lewis, J. *J. Chem Soc., Dalton Trans.* **1983**, 1199. (b) Deeming, A. J.; Peters, R. *J. Organomet. Chem.* **1980**, *202*, C39.

(20) Hausen, H. D.; Gerstner, F.; Schwarz, W. *J. Organomet. Chem.* **1978**, *145*, 277.
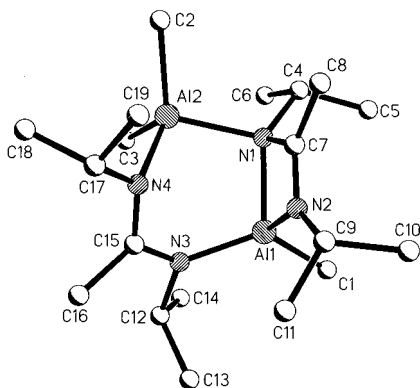
Figure 2. Molecular structure of the {MeC(N^{i}Pr)$_2$}$_2$Al$_2$Me$_3^+$ cation (**2a**$^+$) in [**2a**][B(C$_6$F$_5$)$_4$]. Hydrogen atoms are omitted. Key bond lengths (Å): N(3)−C(15), 1.35(1); N(4)−C(15), 1.31(1); N(1)−C(7), 1.43-(1); N(2)−C(7), 1.27(1); Al(2)−N(1), 2.018(3); Al(1)−N(1), 1.973-(9). Key bond angles (deg): N(1)−Al(1)−N(2), 70.0(4); N(1)−C(7)−N(2), 110.6(9); N(4)−C(15)−N(3), 118.8(9).

cation−anion contacts. The structure of the B(C$_6$F$_5$)$_4^-$ anion is normal. The structure of **2a**$^+$ (Figure 2) is closely analogous to that of **4a**$^+$.

Solution Structure and Dynamic Behavior of [2a][B(C$_6$F$_5$)$_4$] and [2a][MeB(C$_6$F$_5$)$_3$]. The solution behavior of **2a**$^+$ was investigated in detail because the NMR spectra of this cation are simpler and more informative than those of **4a**$^+$, which are complicated by the presence of the Cy groups. The ^{1}H, ^{13}C, ^{11}B, and ^{19}F NMR spectra of [**2a**][B(C$_6$F$_5$)$_4$] are identical to those of [**2a**][MeB(C$_6$F$_5$)$_3$] in CD$_2$Cl$_2$ from −85 to 23 °C, with the exception of the anion resonances. In both cases, resonances characteristic of free anion are observed.[21] In particular, the ^{1}H spectrum of [**2a**][MeB(C$_6$F$_5$)$_3$] in CD$_2$Cl$_2$ contains a broad singlet for the *Me*B(C$_6$F$_5$)$_3^-$ group at δ 0.48, which is characteristic of the free MeB(C$_6$F$_5$)$_3^-$ anion. Thus, cation/anion interactions are not significant for these salts under these conditions.

The ^{1}H and ^{13}C NMR spectra of **2a**$^+$ at −85 °C in CD$_2$Cl$_2$ contain three Al-*Me* signals, two sets of *CMe* signals, eight sets of ^{i}Pr-*CH$_3$* signals, and four sets of ^{i}Pr-*CH* signals. These data are consistent with the C_1 symmetry observed in the solid-state structure. In addition, in the ^{13}C spectrum of **2a**$^+$, one ^{i}Pr-CH resonance and one set of N*CMe*N resonances are significantly broader than the other resonances of these types. This broadening is ascribed to incomplete collapse of ^{13}C−^{14}N coupling and implies that one nitrogen is in a more symmetric environment than the others and hence has a longer quadrupolar relaxation time.[22] This feature is consistent with the presence of one four-coordinate nitrogen and three three-coordinate nitrogens, as observed in the solid state. The Al-*Me* $^1J_{CH}$ values (113, 114, 116 Hz) are consistent with the presence of three terminal Al-*Me* groups. In contrast, the Me-bridged dinuclear cation {(ATI)-AlMe)}$_2$(μ-Me)$^+$ exhibits a large $^1J_{CH}$ value (133 Hz) for the μ-Me group and a normal $^1J_{CH}$ value (118 Hz) for the terminal Me groups.[4b] Thus, on the basis of −85 °C NMR data, it is likely that **2a**$^+$ retains its solid-state structure in CD$_2$Cl$_2$ solution.

As the sample temperature is raised from −85 °C, two dynamic processes can be detected for [**2a**][MeB(C$_6$F$_5$)$_3$] by ^{1}H and ^{13}C NMR that are identified as processes (i) and (ii) in Scheme 2. The lower energy process (i) causes broadening and coalescence of the two highest field Al-*Me* resonances ($T_{coal.}$

= −66 °C in ^{1}H NMR, Figure 3) but does not affect the third (lower field) Al-*Me* resonance. Process (i) also causes the two sets of amidinate N*CMe*N resonances to broaden and coalesce ($T_{coal.}$ = −66 °C in ^{1}H NMR, Figure 4). Additionally, process (i) causes the four ^{i}Pr-*CH* ^{13}C NMR resonances to broaden and collapse as illustrated in Figure 5. The ^{i}Pr-*CH* line shapes could only be simulated adequately by assuming a pairwise exchange of resonances 1 and 4 and of resonances 2 and 3 in Figure 5.[23] These results indicate that process (i) permutes the two amidinate ligands of **2a**$^+$ but does not permute the two ends of a given amidinate ligand. The most reasonable mechanism for this process (Scheme 2) involves a reversible slippage of the μ-η^1,η^2 amidinate to a μ-η^1,η^1 bonding mode and the formation of intermediate species **C**. Species **C** has C_{2v} symmetry as drawn in Scheme 2 but may well adopt a puckered C_s-symmetric structure analogous to that of ({MeC(NMe)$_2$}AlMe$_2$)$_2$.[20] The two high-field Al-*Me* resonances (δ −0.54, −0.75) are assigned to the Al*Me$_2$* unit, and the low-field Al-*Me* resonance (δ −0.17) is assigned to the Al*Me* unit of **2a**$^+$. The free energy barriers for process (i) calculated from the Al-*Me* and N*CMe*N ^{1}H NMR line shapes and the N*C*MeN ^{13}C NMR line shapes are identical ($\Delta G^\ddagger$ = 9.5(7) kcal/mol).[24] Activation parameters for process (i) were obtained from an Eyring plot based on rate constants determined from simulations of the N*CMe*N region of the ^{1}H NMR spectrum (Figure 6, $\Delta H^\ddagger$ = 9.9(5) kcal/mol; $\Delta S^\ddagger$ = 0(3) eu).[25,26] The $\Delta H^\ddagger$ value for process (i) is lower than the enthalpies of Al−N dissociation reported for R$_3$N·AlR$_3$ amine adducts ($\Delta H \approx$ 20−30 kcal/mol).[27] Process (i) is related to the intramolecular exchange of μ-η^1,η^1 amidinate and chelating amidinate groups in Pd bis-amidinate species.[28]

(22) (a) The effect of coupling to quadrupolar nuclei (e.g., ^{14}N, 99.36% abundance, I = 1) on the spectra of spin $^1/_2$ nuclei is described in the following: Harris, R. K. *Nuclear Magnetic Spectroscopy*; Longman Scientific & Technical: Essex, UK, 1986; pp 139−140. In the case of ^{13}C−^{14}N coupling, the ^{13}C line shape is determined by the product $T_{1,^{14}N} \times J_{^{13}C−^{14}N}$. When $10\pi T_{1,^{14}N} \times J_{^{13}C−^{14}N} = 1$, the ^{13}C−^{14}N coupling is completely collapsed, and a sharp singlet is observed for the ^{13}C NMR resonance. Increasing the $T_{1,^{14}N} \times J_{^{13}C−^{14}N}$ product decreases the extent of collapse of ^{13}C−^{14}N coupling; a broad singlet is observed for intermediate values (i.e., $2 < 10\pi T_{1,^{14}N} \times J_{^{13}C−^{14}N} < 10$), and a triplet is observed when $T_{1,^{14}N} \times J_{^{13}C−^{14}N} > 20$. For **2a**$^+$, the broadening of one ^{i}Pr-CH resonance (δ 50.3, $\Delta\nu$ = 12 Hz vs $\Delta\nu$ = 7 Hz (average) for the other ^{i}Pr-CH resonances) and of one set of N*CMe*N resonances (δ 179.4, $\Delta\nu$ = 10 Hz and δ 14.1, $\Delta\nu$ = 16 Hz vs $\Delta\nu$ = 6 and 8 Hz (average) for the other N*CMe*N resonances of the same types) is ascribed to a larger $T_{1,^{14}N}$ value for the four-coordinate nitrogen vs the three-coordinate nitrogens. (b) Higher symmetry at N dramatically increases $T_{1,^{14}N}$. For example, $T_{1,^{14}N} \geq 2000$ ms for [NEt$_4$]I but $T_{1,^{14}N}$ = 38 ms for NH$_3$. See: Lehn, J. M.; Kintzinger, J. P. In *Nitrogen NMR*; Witanowski, M., Webb, G. A., Eds.; Plenum: London, 1973; Chapter 3, pp 124−127.

(23) Note that the difference in the line widths of the four ^{i}Pr-CH signals at −85 °C does not complicate the simulation of the spectra.

(24) Barriers for process (i) were calculated from the coalescence of the Al*Me$_2$*, N*CMe*N, and N*C*MeN resonances using standard formulas for a two−site, equal population exchange process: i.e., $T_{coal.}$ = coalescence temperature; $k_{coal.}$ = exchange rate constant at $T_{coal.}$ = (2.22)($\Delta\nu$); $\Delta G^\ddagger$ = (4.576)$T_{coal.}$(10.32 + log($T_{coal.}/k_{coal.}$)). For ^{1}H NMR: Al*Me$_2$* coalescence, $\Delta\nu$ = 74.2 Hz, $k_{coal.}$ = 165 s^{-1}, $T_{coal.}$ = 207(2) K, $\Delta G^\ddagger$ = 9.5(7) kcal/mol; N*CMe*N coalescence, $\Delta\nu$ = 63.7 Hz, $k_{coal.}$ = 142 s^{-1}, $T_{coal.}$ = 207(2) K, $\Delta G^\ddagger$ = 9.5(7) kcal/mol. For ^{13}C NMR: Al*Me$_2$* coalescence, $\Delta\nu$ = 254.6 Hz, $k_{coal.}$ = 565 s^{-1}, $T_{coal.}$ = 217(2) K, $\Delta G^\ddagger$ = 9.5(7) kcal/mol; N*CMe*N coalescence, $\Delta\nu$ = 53.9 Hz, $k_{coal.}$ = 120 s^{-1}, $T_{coal.}$ = 203(2) K, $\Delta G^\ddagger$ = 9.5(7) kcal/mol; N*C*MeN coalescence, $\Delta\nu$ = 268.1 Hz, $k_{coal.}$ = 595 s^{-1}, $T_{coal.}$ = 217(2) K, $\Delta G^\ddagger$ = 9.5(7) kcal/mol.

(25) The activation parameters were obtained from the Eyring equation: ln(k/T) = ($-\Delta H^\ddagger/R$)/T + 23.76 + $\Delta S^\ddagger/R$, using a least-squares fit of ln(k/T) vs 1/T ($m = -\Delta H^\ddagger/R$, b = 23.76 + $\Delta S^\ddagger/R$). (b) The uncertainties in m and b were used to estimate the uncertainties in $\Delta H^\ddagger$ and $\Delta S^\ddagger$ by standard error propagation methods: $(\sigma_{\Delta H\ddagger})^2 = (-R)^2(\sigma_m)^2$, and $(\sigma_{\Delta S\ddagger})^2 = (-R)^2-(\sigma_b)^2$.[26]

(26) Skoog, D. A.; Leary, J. J. *Principles of Instrumental Analysis*, 4th ed.; Saunders College: New York, 1992; pp A13−14.

(27) Henrickson, C. H.; Duffy, D.; Eyman, D. P. *Inorg. Chem.* **1968**, *7*, 1047.

(21) (a) The ^{13}C, ^{11}B, and ^{19}F NMR spectra for the B(C$_6$F$_5$)$_4^-$ anion of [**2a**][B(C$_6$F$_5$)$_4$] are identical to those for [Ph$_3$C][B(C$_6$F$_5$)$_4$]. (b) The ^{1}H, ^{13}C, ^{11}B, and ^{19}F NMR spectra for the MeB(C$_6$F$_5$)$_3^-$ anion of [**2a**][MeB(C$_6$F$_5$)$_3$] are identical to those for [NBu$_3$(CH$_2$Ph)][MeB(C$_6$F$_5$)$_3$].

Scheme 2

C, M = Al
D, M = Ga

C, M = Al
D, M = Ga
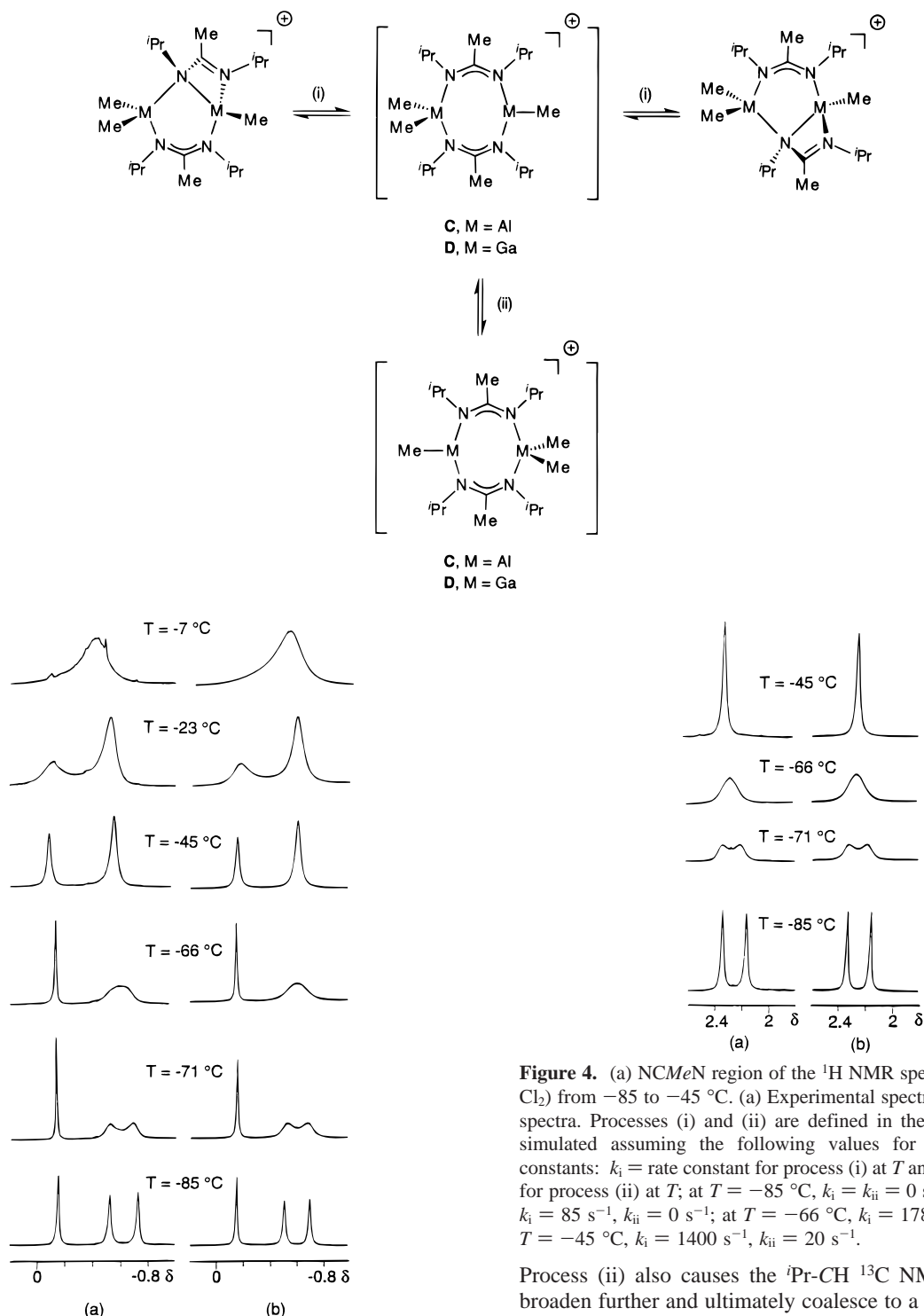
Figure 3. Al-*Me* region of the ^{1}H NMR spectrum of **2a**$^+$ (CD$_2$Cl$_2$) from −85 to −7 °C. (a) experimental spectra and (b) simulated spectra. Processes (i) and (ii) are defined in the text. Spectra were simulated assuming the following values for the exchange rate constants: k_i = rate constant for process (i) at *T* and k_{ii} = rate constant for process (ii) at *T*; at *T* = −85 °C, $k_i = k_{ii} = 0$ s^{-1}; *T* = −71 °C: $k_i = 85$ s^{-1}, $k_{ii} = 0$ s^{-1}; at *T* = −66 °C, $k_i = 178$ s^{-1}, $k_{ii} = 0$ s^{-1}; at *T* = −45 °C, $k_i = 1400$ s^{-1}, $k_{ii} = 20$ s^{-1}; at *T* = −23 °C, $k_i = 12\,400$ s^{-1}, $k_{ii} = 150$ s^{-1}; at *T* = −7 °C, $k_i = 45\,000$ s^{-1}, $k_{ii} = 530$ s^{-1}.

Above −50 °C, a second, higher energy process (process (ii) in Scheme 2) is detected for [**2a**][MeB(C$_6$F$_5$)$_3$] which causes the Al*Me*$_2$ and Al*Me* resonances to broaden and ultimately coalesce to a singlet ($T_{\text{coal.}}$ = −12 °C in ^{1}H NMR, Figure 3).

Figure 4. (a) NC*Me*N region of the ^{1}H NMR spectrum of **2a**$^+$ (CD$_2$-Cl$_2$) from −85 to −45 °C. (a) Experimental spectra and (b) simulated spectra. Processes (i) and (ii) are defined in the text. Spectra were simulated assuming the following values for the exchange rate constants: k_i = rate constant for process (i) at *T* and k_{ii} = rate constant for process (ii) at *T*; at *T* = −85 °C, $k_i = k_{ii} = 0$ s^{-1}; at *T* = −71 °C, $k_i = 85$ s^{-1}, $k_{ii} = 0$ s^{-1}; at *T* = −66 °C, $k_i = 178$ s^{-1}, $k_{ii} = 0$ s^{-1}; at *T* = −45 °C, $k_i = 1400$ s^{-1}, $k_{ii} = 20$ s^{-1}.

Process (ii) also causes the ^{i}Pr-*C*H ^{13}C NMR resonances to broaden further and ultimately coalesce to a singlet at ca. −56 °C, as illustrated in Figure 5. Process (ii) thus permutes all three Al-*Me* groups and permutes the ends of the amidinate ligands, and it must therefore involve exchange of the Me groups between the Al centers. A reasonable mechanism for this process (Scheme 2) is the formation of intermediate **C** followed by migration of a Me group from the *Al*Me$_2$ center to the *Al*Me center. The free energy barrier for process (ii), $\Delta G^{\ddagger} = 11.7(3)$ kcal/mol,[29] was calculated from the Al-*Me* ^{1}H NMR line shape changes. This value is intermediate between the barriers for bridge/terminal Me exchange in Al$_2$Me$_6$ (15.4(2) kcal/mol in toluene)[30] and {(ATI)AlMe)}$_2$(μ-Me)$^+$ ($\Delta G^{\ddagger} = 8.5(4)$ kcal/mol

(28) Barker, J.; Cameron, N.; Kilner, M.; Mahoud, M. M.; Wallwork, S. C. *J. Chem. Soc., Dalton Trans.* **1986**, 1359.
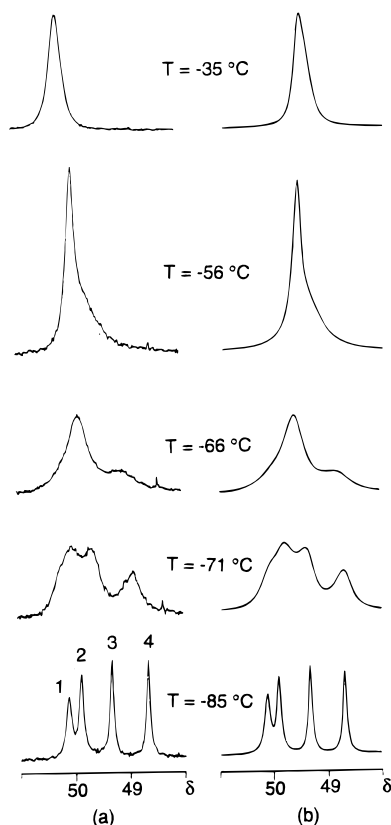
Figure 5. (a) ^{i}Pr-*CH* region of the ^{13}C{^{1}H} spectrum of **2a**$^{+}$ (CD$_2$Cl$_2$) from −85 to −35 °C. (a) Experimental spectra and (b) simulated spectra. Processes (i) and (ii) are defined in the text. Spectra were simulated assuming the following values for the exchange rate constants: k_i = rate constant for process (i) at T and k_{ii} = rate constant for process (ii) at T; at T = −85 °C, k_i = k_{ii} = 0 s^{-1}; at T = −71 °C, k_i = 85 s^{-1}, k_{ii} = 0 s^{-1}; at T = −66 °C, k_i = 178 s^{-1}, k_{ii} = 0 s^{-1}; at T = −56 °C, k_i = 605 s^{-1}, k_{ii} = 7 s^{-1}; at T = 35 °C, k_i = 2500 s^{-1}, k_{ii} = 63 s^{-1}. The apparent monotonic shift of resonances 1−4 to lower field as the temperature is increased was not incorporated in the simulations.

in CD$_2$Cl$_2$).[31] The activation parameters for process (ii) were obtained from an Eyring plot based on rate constants determined from simulation of the Al-*Me* region of the ^{1}H NMR spectrum (Figure 7, $\Delta H^{\ddagger}$ = 9.7(5) kcal/mol; $\Delta S^{\ddagger}$ = −9(2) eu).

The possibility that the dynamic behavior of **2a**$^{+}$ involves dissociation of **2a**$^{+}$ into the base-free {MeC(N^{i}Pr)$_2$}AlMe^{+} cation and **1a** can be ruled out by NMR observations. Thus, the ^{1}H NMR spectrum of [**2a**][MeB(C$_6$F$_5$)$_3$] in CD$_2$Cl$_2$ at 23 °C in the presence of 1 equiv of **1a** contains sharp resonances for [**2a**][MeB(C$_6$F$_5$)$_3$] and **1a** in a 1/1 ratio. This result establishes that intermolecular exchange of [**2a**][MeB(C$_6$F$_5$)$_3$] and **1a** is slow on the NMR time scale under conditions where processes (i) and (ii) are both rapid on the NMR time scale. The lack of intermolecular [**2a**][MeB(C$_6$F$_5$)$_3$]/**1a** exchange

(29) The free energy barrier for process (ii) was calculated from the coalescence of the Al*Me*$_2$ and Al*Me* ^{1}H NMR resonances using the graphical method for a two-site, unequal population exchange process described in the following: Shanan-Atidi, H.; Bar-Eli, K. H. *J. Phys. Chem.* **1970**, *74*, 961. $T_{coal.}$ = 261(2) K, $k_{coal.}$ = 522 s^{-1}, $\Delta G^{\ddagger}$ = 11.7(3) kcal/mol. Similar estimates for the exchange barrier for process (ii) were obtained from the analysis of the line broadening of the Al*Me* resonance between 223 and 239 K ($\Delta G^{\ddagger}$ ≈ 11.7 kcal/mol).

(30) Ham, N. S.; Mole, T. In *Progress in NMR Spectroscopy*; Emsley, J. W., Feeney, J., Sutcliffe, V., Eds.; Pergamon: New York, NY, 1969; Vol. 4, p 128.

(31) The free energy barrier for the bridge/terminal Me exchange in {(ATI)AlMe)}$_2$(μ-Me)$^{+}$ was estimated from the line broadening of the bridging Al-*Me* resonance at 190 K ($\Delta G^{\ddagger}$ ≈ 8.5(4) kcal/mol).
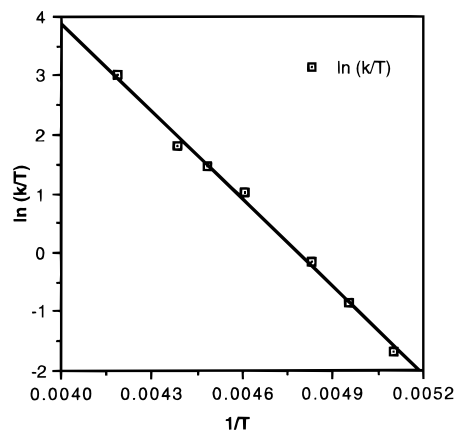
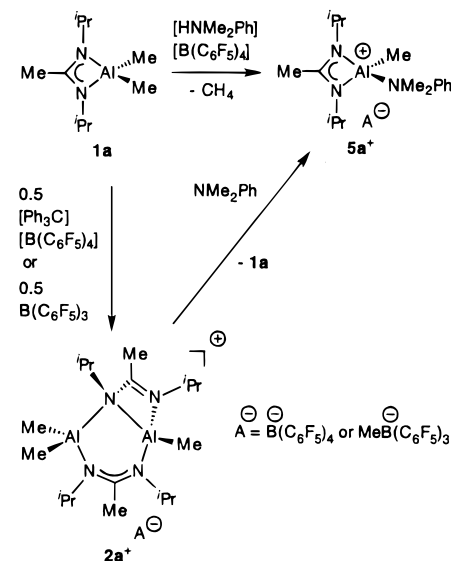**Figure 6.** Eyring Plot for process (i) for **2a**$^{+}$.
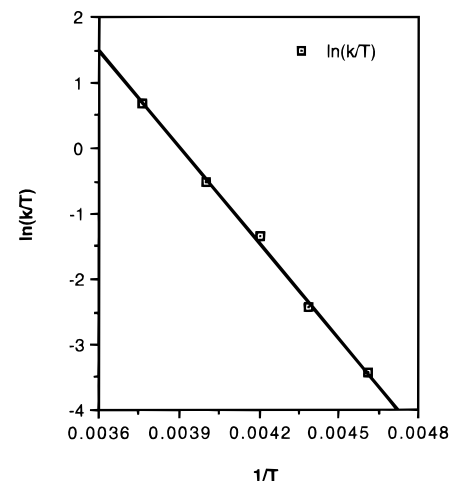
Figure 7. Eyring Plot for process (ii) for **2a**$^{+}$.

Scheme 3

contrasts with the fast intermolecular exchange observed for {(ATI)AlMe)}$_2$(μ-Me)$^{+}$ and (ATI)AlMe$_2$ at 23 °C.[4b]

Reaction of [2a][MeB(C$_6$F$_5$)$_3$] with Lewis Bases. The reaction of [**2a**][MeB(C$_6$F$_5$)$_3$] with 1 equiv of NMe$_2$Ph in CD$_2$-Cl$_2$ (12 h, 23 °C) yields a 1/1 mixture of the amine adduct [{MeC(N^{i}Pr)$_2$}Al(Me)(NMe$_2$Ph)][MeB(C$_6$F$_5$)$_3$] (**5a**][MeB-(C$_6$F$_5$)$_3$]) and **1a** (85% by ^{1}H NMR, Scheme 3). [**5a**][MeB-(C$_6$F$_5$)$_3$] is stable in CD$_2$Cl$_2$ at 23 °C for several days and is thus more robust than [**2a**][MeB(C$_6$F$_5$)$_3$]. The ^{1}H and ^{13}C NMR

spectra of [**5a**][MeB(C_6F_5)$_3$] (CD$_2$Cl$_2$) contain characteristic resonances for the free MeB(C_6F_5)$_3^-$ anion along with one Al-*Me* signal, one NC*Me*N signal, and two ^{i}Pr-*CH$_3$* signals, which is consistent with C_s symmetry at Al. The coordination of NMe$_2$-Ph is also evidenced by ^{1}H and ^{13}C NMR. The *o*-Ph and *p*-Ph ^{1}H NMR resonances (δ 7.47, 7.51) and the N*Me* ^{13}C NMR resonance (δ 46.0) of the coordinated NMe$_2$Ph are shifted downfield from the corresponding resonances of free NMe$_2$-Ph.[32] The identity of **5a**$^+$ was confirmed by generation of [**5a**]-[B(C_6F_5)$_4$] by a protonolysis route. The reaction of **1a** with 1 equiv of [HNMe$_2$Ph][B(C_6F_5)$_4$] in CD$_2$Cl$_2$ (15 min, 23 °C) yields [**5a**][B(C_6F_5)$_4$] (100% by ^{1}H NMR, Scheme 3) and methane.[33]

Reaction of {MeC(N^{i}Pr)$_2$}GaMe$_2$ (1b) with Cationic Activators. The reaction of **1b** with 0.5 equiv of B(C_6F_5)$_3$ in C_6D_5Cl (15 min, 23 °C) yields the dinuclear cation {MeC(N^i-Pr)$_2$}$_2$Ga$_2$Me$_3^+$ (**2b**$^+$) as the MeB(C_6F_5)$_3^-$ salt (100% by ^{1}H NMR vs an internal standard, Scheme 1). [**2b**][MeB(C_6F_5)$_3$] does not undergo further reaction with excess B(C_6F_5)$_3$ at 23 °C and is more stable in C_6D_5Cl at 23 °C ($t_{1/2} \approx 5$ d) than its Al analogue [**2a**][MeB(C_6F_5)$_3$]. The salt [**2b**][MeB(C_6F_5)$_3$] was isolated as an analytically pure colorless solid (71%) by generation in 10/1 hexane/CH$_2$Cl$_2$ mixture followed by several pentane washes. The variable-temperature NMR data for **2b**$^+$ parallel the data for **2a**$^+$ and establish that the two species have analogous structures and dynamic properties.[34]

In contrast, **1b** reacts readily with [Ph$_3$C][B(C_6F_5)$_4$] in C_6D_5-Cl (10 min, 23 °C), but neither **2b**$^+$ nor Ph$_3$CCH$_3$ is observed as products. Similarly, **1b** reacts with [HNMe$_2$Ph][B(C_6F_5)$_4$] in C_6D_5Cl (1 h, 23 °C), but neither {MeC(N^{i}Pr)$_2$}Ga(Me)(NMe$_2$-Ph)$^+$ nor CH$_4$ is observed. Thus, in contrast to the case for the corresponding Al reactions, it appears that Ph$_3$C$^+$ and HNMe$_2$-Ph$^+$ attack the Ga amidinate unit rather than the Ga−Me bonds of **1b**.

Reaction of {^{t}BuC(N^{i}Pr)$_2$}AlMe$_2$ (6a) with [Ph$_3$C][B(C_6F_5)$_4$]. The methyl abstraction chemistry of the ^{t}Bu-substituted amidinate complexes {^{t}BuC(N^{i}Pr)$_2$}MMe$_2$ (M = Al, **6a**; M = Ga, **6b**) was investigated in an effort to disfavor the formation of dinuclear Al species. Replacing the *Me*C unit of **1a** by a ^{t}BuC unit increases the steric interactions between the amidinate substituents, which in turn increases the steric crowding at the metal center.[17]

The reaction of **6a** with 0.5 equiv of [Ph$_3$C][B(C_6F_5)$_4$] in C_6D_5Cl (10 min, 23 °C) yields a 1/1 mixture of Ph$_3$CCH$_3$ and the dinuclear species [{^{t}BuC(N^{i}Pr)$_2$}AlMe·{^{t}BuC(N^{i}Pr)$_2$}-AlMe$_2$]$^+$ (**7a**$^+$) as the B(C_6F_5)$_4^-$ salt ([**7a**][B(C_6F_5)$_4$], 90% by ^{1}H NMR, Scheme 4).[35] [**7a**]-[B(C_6F_5)$_4$] does not undergo further reaction with excess [Ph$_3$C][B(C_6F_5)$_4$] at 23 °C in C_6D_5Cl. [**7a**]-[B(C_6F_5)$_4$] decomposes in C_6D_5Cl ($t_{1/2} \approx 3$ h, 23 °C) and C_6D_6 ($t_{1/2} \approx 7$ h, 23 °C) and therefore could not be isolated in pure form.

Scheme 4

The composition of [**7a**][B(C_6F_5)$_4$] was established by chemical derivatization. The reaction of [**7a**][B(C_6F_5)$_4$] with 1 equiv of NMe$_2$Ph in CD$_2$Cl$_2$ (10 min, 23 °C) yields a 1/1 mixture of **6a** and the amine adduct [{^{t}BuC(N^{i}Pr)$_2$}Al(Me)(NMe$_2$Ph)]-[B(C_6F_5)$_4$] ([**8a**][B(C_6F_5)$_4$], Scheme 4).[36] Interestingly, this reaction is much faster than the reaction of **2a**$^+$ and NMe$_2$Ph (12 h, 23 °C). The ^{1}H and ^{13}C NMR data for [**8a**][B(C_6F_5)$_4$] are similar to those for [**5a**][B(C_6F_5)$_4$].

The ^{11}B and ^{19}F NMR spectra of [**7a**][B(C_6F_5)$_4$] in C_6D_5Cl establish that the B(C_6F_5)$_4^-$ anion is free in solution. The ^{1}H and ^{13}C NMR spectra of [**7a**][B(C_6F_5)$_4$] are unchanged between −60 and 60 °C, indicating that, unlike **2a**$^+$, **7a**$^+$ is not fluxional over this temperature range.[37] The ^{1}H and ^{13}C NMR spectra of [**7a**][B(C_6F_5)$_4$] contain three Al-*Me* signals, two ^{t}Bu signals, and four ^{i}Pr-*CH* signals, which is consistent with the presence of two inequivalent Al centers and overall C_1 symmetry. These data do not allow a definitive structural assignment for [**7a**]-[B(C_6F_5)$_4$]. However, the facts that (i) the ^{1}H NMR Al-*Me* chemical shifts of **7a**$^+$ are very similar (δ −0.34, −0.39, and −0.42) whereas those for **2a**$^+$ are very different (δ −0.17, −0.54 and −0.75), (ii) **7a**$^+$ is rigid in solution while **2a**$^+$ is fluxional, and (iii) **7a**$^+$ reacts much more rapidly with NMe$_2$Ph than does **2a**$^+$ suggest that the structure of **7a**$^+$ is different from those of **2a**$^+$ and **4a**$^+$. In fact, the NMR spectra of **7a**$^+$ are nearly identical to those of the analogous dinuclear Ga cation [{^{t}BuC-(N^{i}Pr)$_2$}GaMe·{^{t}BuC(N^{i}Pr)$_2$}GaMe$_2$]$^+$ (**7b**$^+$), in which the two metal centers are connected by a μ-η^1,η^2 bridging amidinate (vide infra). Thus, it is likely that **7a**$^+$ adopts a similar structure, as illustrated in Scheme 4.

Reaction of {^{t}BuC(N^{i}Pr)$_2$}GaMe$_2$ (6b) with [Ph$_3$C]-[B(C_6F_5)$_4$]. The reaction of **6b** with 0.5 equiv of [Ph$_3$C]-[B(C_6F_5)$_4$] in C_6D_5Cl (15 min, 23 °C) yields the dinuclear cation [{^{t}BuC(N^{i}Pr)$_2$}GaMe·{^{t}BuC(N^{i}Pr)$_2$}GaMe$_2$]$^+$ (**7b**$^+$) as the B(C_6F_5)$_4^-$ salt ([**7b**][B(C_6F_5)$_4$], 100% by ^{1}H NMR vs an internal

(32) Data for NMe$_2$Ph. ^{1}H NMR (CD$_2$Cl$_2$): δ 7.23 (t, ^3J = 7.5, 2H, *m*-Ph), 6.75 (d, ^3J = 7.6, 2H, *o*-Ph), 6.71 (t, ^3J = 7.2, 1H, *p*-Ph), 2.95 (s, 6H, N*Me*). ^{13}C NMR (CD$_2$Cl$_2$): δ 151.3 (*ipso*-Ph), 129.4 (*Ph*), 116.8 (*Ph*), 113.0 (*Ph*), 40.7 (N*Me*).

(33) The ^{1}H and ^{13}C NMR data for [**5a**][B(C_6F_5)$_4$] are identical to those for [**5a**][MeB(C_6F_5)$_3$] except for the anion resonances.

(34) (a) In particular, the widely divergent Ga-*Me* ^{1}H NMR chemical shifts for **2b**$^+$ at −85 °C (δ 0.43, −0.04, −0.27) parallel those observed for **2a**$^+$ at −85 °C (δ −0.17, −0.54, −0.75). (b) The *Me* line shape changes for **2b**$^+$ between −85 and 23 °C parallel those for **2a**$^+$ and are consistent with the occurrence of processes (i) and (ii) via the intermediate **D**, as illustrated in Scheme 2. (c) The free energy barrier for process (ii) ($\Delta G^{\ddagger}$ = 14.8(4) kcal/mol) calculated from the Ga-*Me* ^{1}H NMR line shape changes for **2b**$^+$ is higher than that for **2a**$^+$ ($\Delta G^{\ddagger}$ = 11.7(3) kcal/mol).

(35) Both the addition of [Ph$_3$C][B(C_6F_5)$_4$] to a solution of **6a** and the addition of **6a** to a solution of [Ph$_3$C][B(C_6F_5)$_4$] yield [**7a**][B(C_6F_5)$_4$] (90% by ^{1}H NMR).

(36) The generation of [**8a**][B(C_6F_5)$_4$] by the reaction of **6a** with [HNMe$_2$-Ph][B(C_6F_5)$_4$] confirmed this assignment.

(37) (a) Due to the low stability of [**7a**][B(C_6F_5)$_4$] in CD$_2$Cl$_2$, NMR spectra were recorded in CD$_2$Cl$_2$ from −60 to −30 °C and C_6D_5Cl from −30 to 60 °C. (b) [**7a**][B(C_6F_5)$_4$] rapidly decomposes at 60 °C ($t_{1/2}$ = 15 min), which precluded NMR studies at higher temperatures. (c) Additionally, the ^{1}H and ^{13}C NMR spectra of a 1/1 mixture of [**7a**][B(C_6F_5)$_4$] and **6a** at 23 °C in C_6D_5Cl contain sharp resonances of the two complexes in a 1/1 ratio, which shows that intermolecular exchange between [**7a**][B(C_6F_5)$_4$] and **6a** is slow on the NMR time scale under these conditions.
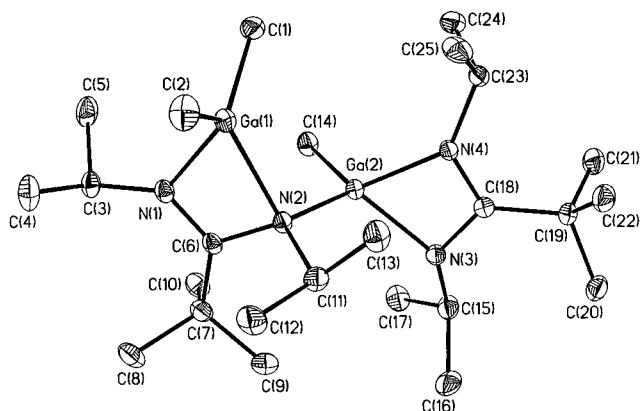
Figure 8. Molecular structure of the {^{t}BuC(N^{i}Pr)$_2$}GaMe·{^{t}BuC(N^i-Pr)$_2$}GaMe$_2^+$ cation (**7b$^+$**) in [**7b**][B(C$_6$F$_5$)$_4$]. Hydrogen atoms are omitted.

Chart 3

E
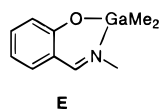
standard, Scheme 4).[38] [**7b**][B(C$_6$F$_5$)$_4$] does not undergo further reaction with excess [Ph$_3$C][B(C$_6$F$_5$)$_4$] at 23 °C in C$_6$D$_5$Cl. Unlike the Al analogue [**7a**][B(C$_6$F$_5$)$_4$], [**7b**][B(C$_6$F$_5$)$_4$] is stable at 23 °C in C$_6$D$_5$Cl for several days and was isolated as an analytically pure yellow solid (64%) by generation in benzene followed by several hexane and pentane washes. [**7b**][B(C$_6$F$_5$)$_4$] was obtained as pale yellow crystals by crystallization from a mixed solvent system (10/10/1 hexane/pentane/C$_6$D$_5$Cl, see Experimental Section), and its structure was determined by X-ray crystallography.

Molecular Structure of [7b][B(C$_6$F$_5$)$_4$]. [**7b**][B(C$_6$F$_5$)$_4$] crystallizes as discrete **7b$^+$** and B(C$_6$F$_5$)$_4^-$ ions with no close cation−anion contacts. The structure of the B(C$_6$F$_5$)$_4^-$ anion is normal. The molecular structure of **7b$^+$** is illustrated in Figure 8. **7b$^+$** has overall C_1 symmetry and is an adduct of {^{t}BuC(N^i-Pr)$_2$}GaMe$^+$ and {^{t}BuC(N^{i}Pr)$_2$}GaMe$_2$. The two Ga centers are linked by a μ-η^1,η^2 bridging amidinate ligand (N(1)−C(6)−N(2)) through N(2). The μ-η^1,η^2 amidinate unit is very similar to those in the dinuclear Al cations **2a$^+$** and **4a$^+$**. The C(6)−N(1) and C(6)−N(2) distances (1.285(3) and 1.459(3) Å) are significantly different, indicating that the π-bonding within the N−C−N unit is localized. N(1) bonds as an imine to Ga(1). The Ga(1)−N(1) distance (2.007(2) Å) is comparable to those observed in neutral Ga imine complexes (e.g., *N*-methylsalicy-laldiminate gallium dimethyl, **E**, Chart 3, 2.019(7) Å).[39]

N(2) bonds to Ga(1) and Ga(2) as an unsymmetrical μ-amide. The Ga(1)−N(2) distance (2.155(2) Å) is similar to those in bulky gallium amine adducts (e.g., Me$_3$Ga(N^{t}BuH$_2$), 2.12(1) Å).[40] The Ga(2)−N(2) distance (2.037(2) Å) is comparable to those in bulky gallium μ-amide complexes, e.g., {Me$_2$Ga(μ-NH(1-Ad))}$_2$ (2.02(4) Å average) and {Me$_2$Ga(μ-NHPh)}$_2$ (2.03(7) Å).[16] The N(1)−C(6)−N(2) angle (108.6(2)°) is similar to those in **2a$^+$** (110.6(9)°) and **4a$^+$** (109.6(1)°).

The two Ga centers in **7b$^+$** adopt distorted tetrahedral geometries similar to those in {^{t}BuC(NR′)$_2$}GaMe$_2$ (R′ = Cy,

^{t}Bu) complexes.[41] The amidinate that chelates Ga(2) (N(4)−C(18)−N(3)) is normal; i.e., it is symmetrically bonded to Ga-(2), it exhibits delocalized NCN π-bonding, and the N(4)−C(18)−N(3) angle (109.2(2)°) is in the expected range. The Ga−C bond distances (1.950(3) Å average) are slightly shorter than those in {^{t}BuC(NR′$_2$)$_2$}GaMe$_2$ (R′ = Cy, ^{t}Bu; 1.98(2) Å average)[41] and [Me$_2$Ga(NH$_2$^{t}Bu)$_2$]Br (1.97(6) Å average).[42]

Solution Structure of [7b][B(C$_6$F$_5$)$_4$]. The ^{1}H, ^{13}C, ^{11}B, and ^{19}F NMR spectra of [**7b**][B(C$_6$F$_5$)$_4$] in CD$_2$Cl$_2$ are essentially unchanged between −60 and 60 °C and indicate that the B(C$_6$F$_5$)$_4^-$ anion is free in solution and that the **7b$^+$** cation is not fluxional over this temperature range.[43] The ^{1}H and ^{13}C NMR spectra of **7b$^+$** contain three Ga-*Me* resonances at very similar chemical shifts (δ 0.55, 0.45, 0.35), two sets of *C^{t}Bu* resonances, four sets of ^{i}Pr-*CH* resonances, and eight ^{i}Pr-*CH$_3$* resonances.[44] The Ga*Me* $^1J_{CH}$ values for **7b$^+$** (125, 123, 123 Hz) are consistent with the presence of three terminal Ga-*Me* groups. These data are consistent with the C_1-symmetric structure observed for **7b$^+$** in the solid state. The rigidity of **7b$^+$** in solution and the similarity of the Ga-*Me* ^{1}H NMR chemical shifts parallel the properties of the Al analogue **7a$^+$** but contrast with the dynamic behavior and divergent Al-*Me* and Ga-*Me* ^{1}H NMR chemical shifts observed for **2a$^+$** and **2b$^+$**. Thus, it is clear that **7b$^+$** and **7a$^+$** adopt analogous structures.

Reaction of [7b][B(C$_6$F$_5$)$_4$] with NMe$_2$Ph. The reaction of [**7b**][B(C$_6$F$_5$)$_4$] with 1 equiv of NMe$_2$Ph in C$_6$D$_5$Cl (15 min, 23 °C) yields a 1/1 mixture of **6b** and the amine adduct [{^{t}BuC-(N^{i}Pr)$_2$}Ga(Me)(NMe$_2$Ph)][B(C$_6$F$_5$)$_4$] ([**8b**][B(C$_6$F$_5$)$_4$], Scheme 4).[45] The ^{1}H and ^{13}C NMR spectra of [**8b**][B(C$_6$F$_5$)$_4$] (C$_6$D$_5$Cl) are very similar to those of [**8a**][B(C$_6$F$_5$)$_4$].

Reaction of {^{t}BuC(NR′)$_2$}AlMe$_2$ (R′ = ^{i}Pr, 6a; R′ = Cy, 10a) with B(C$_6$F$_5$)$_3$. Initial studies suggested that the reaction of **6a** or **10a** with B(C$_6$F$_5$)$_3$ yields {^{t}BuC(NR′)$_2$}Al(Me)(MeB-(C$_6$F$_5$)$_3$) ion pairs.[4a] However, further studies have shown that these reactions are more complicated. The reaction of **6a** with 1 equiv of B(C$_6$F$_5$)$_3$ in C$_6$D$_5$Cl or CD$_2$Cl$_2$ (20 min, 23 °C) yields a 1/1 mixture of {^{t}BuC(N^{i}Pr)$_2$}Al(Me)(C$_6$F$_5$) (**9a**) and MeB-(C$_6$F$_5$)$_2$ (100% by ^{1}H NMR, Scheme 5). The **9a**/MeB(C$_6$F$_5$)$_2$ mixture was characterized by ^{1}H, ^{11}B, and ^{19}F NMR. The ^{13}C and ^{19}F NMR spectra of the mixture each contain two sets of C$_6$F$_5$ signals (2/1 intensity ratio in ^{19}F NMR). The ^{1}H and ^{13}C NMR spectra for **9a** contain one Al-*Me* resonance, one ^{i}Pr-*CH* resonance, and two ^{i}Pr-*CH$_3$* resonances, which is consistent with C_s symmetry at Al. The NMR data for MeB(C$_6$F$_5$)$_2$ are consistent with literature data (^{11}B NMR, δ 72).[46]

The reaction of **6a** and B(C$_6$F$_5$)$_3$ at low temperature in CD$_2$-Cl$_2$ was monitored by ^{11}B and ^{1}H NMR to determine if the formation of cationic complexes precedes the formation of **9a**

(41) Dagorne, S.; Young, V. G., Jr.; Jordan, R. F. Manuscript in preparation.

(42) Atwood, D. A.; Jones, R. A.; Cowley, A. H.; Bott, S. G.; Atwood, J. L. *J. Organomet. Chem.* **1992**, *425*, C1.

(43) (a) [**7b**][B(C$_6$F$_5$)$_4$] rapidly decomposes in C$_6$D$_5$Cl at 60 °C ($t_{1/2}$ = 30 min). (b) The ^{1}H NMR spectrum of a 1/1 mixture of [**7b**][B(C$_6$F$_5$)$_4$] and **6b** in CD$_2$Cl$_2$ contains sharp resonances of the two complexes between −60 and 60 °C, which indicates that intermolecular exchange between **7b$^+$** and **6b** is slow on the NMR time scale.

(44) As for **2a$^+$**, the ^{13}C NMR spectrum of **7b$^+$** contains one set of N*C^{t}Bu*N resonances and one ^{i}Pr-*CH* resonance that are significantly broader than the other resonances of the same type, which is consistent with the presence of one four-coordinate nitrogen and three three-coordinate nitrogens.

(45) In contrast, the reaction of **6b** with [HNMe$_2$Ph][B(C$_6$F$_5$)$_4$] yields undentified species.

(46) (a) Qian, B.; Ward, D. L.; Smith, M. R. *Organometallics* **1998**, *17*, 3070. For comparison, the ^{11}B NMR resonance for MeBPh$_2$ appears at δ 70.6 in CD$_2$Cl$_2$. See: Wrackmeyer, B.; Nöth, H. *Chem. Ber.* **1976**, *109*, 1075.

(38) Slow addition of **6b** to a solution of [Ph$_3$C][B(C$_6$F$_5$)$_4$] and addition of [Ph$_3$C][B(C$_6$F$_5$)$_4$] to a solution of **6b**. Both afford [**7b**][B(C$_6$F$_5$)$_4$] in ca. 64% yield.

(39) Bregadze, V. I.; Furmanova, N. G.; Golubinskaya, L. M.; Kompan, O. Y.; Struchkov, Y. T. *J. Organomet. Chem.* **1980**, *192*, 1.

(40) Atwood, D. A.; Jones, R. A.; Cowley, A. H., Bott, S. G.; Atwood, J. L. *J. Organomet. Chem.* **1993**, *453*, 24.

Scheme 5

Figure 9. Molecular structure of {^{t}BuC(NCy)$_2$}Al(Me)(C$_6$F$_5$) (**11a**).
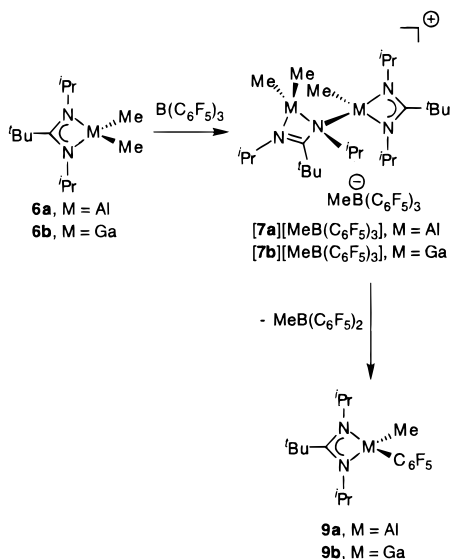
and MeB(C$_6$F$_5$)$_2$. The ^{1}H and ^{11}B NMR spectra of the mixture after 15 min at −60 °C contain characteristic MeB(C$_6$F$_5$)$_3^-$ resonances, which is consistent with the formation of cationic Al species. The ^{1}H NMR spectrum also contains resonances for **7a**$^+$ (ca. 80% by ^{1}H NMR) that are identical to those of [**7a**][B(C$_6$F$_5$)$_4$], and resonances for unidentified species (20% by ^{1}H NMR). Attempts to isolate [**7a**][MeB(C$_6$F$_5$)$_3$] were not successful due to the rapid conversion to **9a** and MeB(C$_6$F$_5$)$_2$ above 0 °C. Thus, the reaction of **7a** with B(C$_6$F$_5$)$_3$ proceeds by initial Me$^-$ abstraction to generate ionic species which decompose by C$_6$F$_5^-$ transfer (Scheme 5). Analogous degradation products were observed in the reaction of the β-diketiminate Al complex {HC(CMeN(p-tolyl)}$_2$AlMe$_2$ and B(C$_6$F$_5$)$_3$,[46] and in group 4 metal complexes.[47]

Similarly, the reaction of {^{t}BuC(NCy)$_2$}AlMe$_2$ (**10a**) with 1 equiv of B(C$_6$F$_5$)$_3$ in CD$_2$Cl$_2$ (20 min, 23 °C) yields a 1/1 mixture of {^{t}BuC(NCy)$_2$Al(Me)(C$_6$F$_5$) (**11a**) and MeB(C$_6$F$_5$)$_2$ (100% by ^{1}H NMR). The ^{1}H NMR data for **11a** are similar to the data for **9a** except for the NCy resonances. In addition, **11a** was characterized by X-ray crystallography, which confirmed the structures of both **11a** and **9a**. The molecular structure of **11a** is illustrated in Figure 9. Compound **11a** adopts a distorted tetrahedral structure similar to that of **10a**.[17] The C$_6$F$_5$ ring is normal. The Al–C$_6$F$_5$ bond distance (Al–C(31), 2.011(3) Å) is longer than the terminal Al–Ph bond distances in Al$_2$Ph$_6$ (1.95(8) Å average).[48] The Al–CH$_3$ bond distance (Al–C(1), 1.941(3) Å) is similar to those of **10a** (1.954(2) Å average).[17]

Reaction of {^{t}BuC(N^{i}Pr)$_2$}GaMe$_2$ (6b) with B(C$_6$F$_5$)$_3$. The reaction of **6b** with 1 equiv of B(C$_6$F$_5$)$_3$ in C$_6$D$_5$Cl (15 min, 23 °C) yields [**7b**][MeB(C$_6$F$_5$)$_3$] (100% by ^{1}H NMR vs an internal standard, Scheme 5) along with 0.5 equiv of unreacted B(C$_6$F$_5$)$_3$. The ^{1}H NMR spectrum of the product mixture contains resonances for [**7b**][MeB(C$_6$F$_5$)$_3$] which are identical to those for [**7b**][B(C$_6$F$_5$)$_4$] except for the anion resonances, and the ^{11}B NMR spectrum contains a resonance at δ −14 characteristic of the MeB(C$_6$F$_5$)$_3^-$ anion and a very broad resonance at δ 61 corresponding to B(C$_6$F$_5$)$_3$.[49] The [**7b**][MeB(C$_6$F$_5$)$_3$]/B(C$_6$F$_5$)$_3$ mixture quantitatively evolves to a 1/1 mixture of {^{t}BuC(N^i-

Pr)$_2$}Ga(Me)(C$_6$F$_5$) (**9b**) and MeB(C$_6$F$_5$)$_2$ after 7 h in C$_6$D$_5$Cl or 12 h in C$_6$D$_6$.[50] Thus, [**7b**][MeB(C$_6$F$_5$)$_3$] is more stable than the Al analogue [**7a**][MeB(C$_6$F$_5$)$_3$] but nevertheless could not be isolated in pure form. The NMR spectra of **9b** are very similar to those of the Al analogues **9a** and **11a**. In addition, the ^{13}C NMR spectrum of **9b** contains a sharp ipso-C$_6$F$_5$ resonance (δ 115.6, t, $^2J_{CF}$ = 45 Hz) showing the presence of a C$_6$F$_5$ group not bound to boron and thus consistent with the presence of a Ga–C$_6$F$_5$ group. In contrast, B-ipso-C$_6$F$_5$ resonances are normally very broad if detected at all.
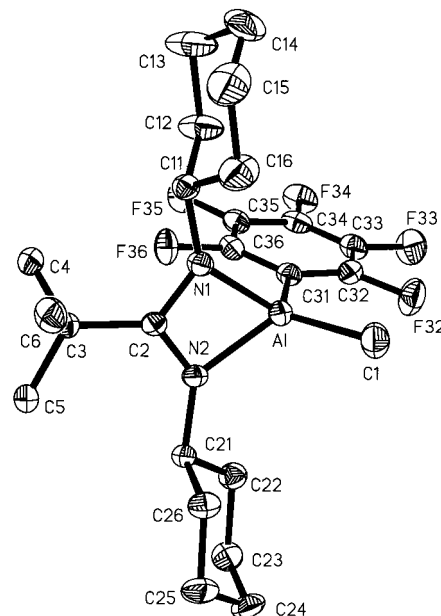
Synthesis and Structure of {^{t}BuC(N^{t}Bu)$_2$}AlMe$_2$ (12a). The difference in structures of **2a**$^+$, **2b**$^+$, and **4a**$^+$ (double amidinate bridging) vs **7a**$^+$ and **7b**$^+$ (single amidinate bridging) suggested that utilization of "super-bulky" amidinate ligands might allow generation of mononuclear cationic Al and Ga species. Accordingly, the synthesis and methyl abstraction chemistry of {^{t}BuC(N^{t}Bu)$_2$}MMe$_2$ (**12a** and **12b**) were investigated.

The ^{t}Bu-amidinate reagent Li[^{t}BuC(N^{t}Bu)$_2$] was generated by the reaction of ^{t}BuLi with ^{t}BuN=C=N^{t}Bu (Et$_2$O, 0 °C) and reacted in situ with 1 equiv of AlMe$_2$Cl (Et$_2$O, 0 °C) to yield {^{t}BuC(N^{t}Bu)$_2$}AlMe$_2$ (**12a**, Scheme 6).[51] Complex **12a** is highly air-sensitive and was isolated as a colorless crystalline solid by sublimation (70 °C, <0.001 mmHg). The ^{1}H and ^{13}C NMR spectra of **12a** (C$_6$D$_6$) at 23 °C are consistent with C$_s$ or higher symmetry at Al. The highest m/e peak in the EI mass spectrum of **12a** corresponds to the [AlMe$_2$]$^+$ ion, which contrasts with the EI mass spectra of **1a**, **3a**, **6a**, and **10a**, which all contain peaks for [{RC(NR')$_2$}AlMe]$^+$ ions.[17] This difference suggests that the bulky ^{t}BuC(N^{t}Bu)$_2^-$ ligand is more labile than the MeC(NR)$_2^-$ (R = ^{i}Pr, Cy) and ^{t}BuC(NR)$_2^-$ (R = ^{i}Pr, Cy) ligands.

The molecular structure of **12a** was determined by X-ray crystallography and is illustrated in Figure 10. Compound **12a** adopts a distorted tetrahedral structure similar to that of **10a**. However, the ^{t}Bu–N–C bond angles in **12a** (139.6(2)° average)

(47) Yang, X.; Stern, C. L.; Marks, T. J. *J. Am. Chem. Soc.* **1994**, *116*, 10015.

(48) Malone, J. F.; McDonald, W. S. *J. Chem. Soc., Dalton Trans.* **1972**, 2646.

(49) A ^{11}B NMR spectrum of B(C$_6$F$_5$)$_3$ in C$_6$D$_5$Cl at 80 °C confirmed this assignment.

(50) [**7b**][MeB(C$_6$F$_5$)$_3$] is also unstable in the absence of B(C$_6$F$_5$)$_3$ in C$_6$D$_5$Cl and is converted to **9b** (10 h, 23 °C, 90% by ^{1}H NMR) and unidentified boron species.

(51) (a) For synthesis of mono-amidinate group 13 dialkyl complexes by salt metathesis routes, see: Kottmair-Maieron, D.; Lechter, R.; Weidlein, J. *Z. Anorg. Allg. Chem.* **1991**, *593*, 111. (b) For the synthesis of **12b**, see ref 41.
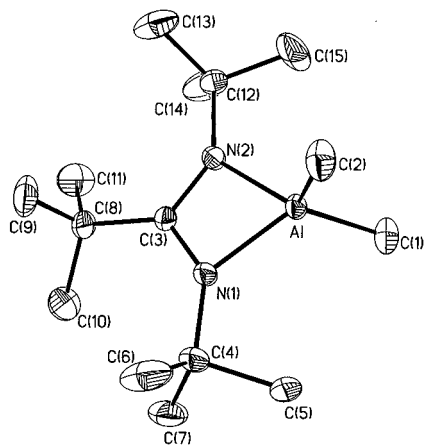
**Figure 10.** Molecular structure of {^{t}BuC(N^{t}Bu)$_2$}AlMe$_2$ (**12a**). Hydrogen atoms are omitted.

Scheme 6
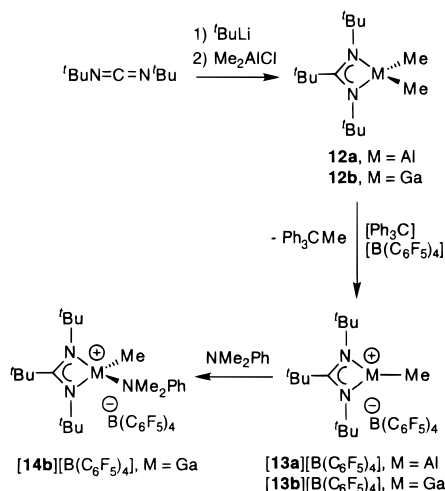
are larger than the corresponding Cy−N−C bond angles in **10a** (131.9(5)° average) due to the severe steric crowding between the ^{t}Bu-C and N-^{t}Bu substituents in **12a**. As a result, the ^{t}Bu−N−Al bond angles in **12a** (127.7(1)° average) are smaller than the Cy−N−Al bond angles in **10a** (133.9(5)° average).

Reaction of {^{t}BuC(N^{t}Bu)$_2$}MMe$_2$ (12a, M = Al; 12b, M = Ga) with [Ph$_3$C][B(C$_6$F$_5$)$_4$]. The reaction of **12a** or **12b** with 1 equiv of [Ph$_3$C][B(C$_6$F$_5$)$_4$] in C$_6$D$_5$Cl (10 min, 23 °C) yields a 1/1 mixture of [{^{t}BuC(N^{t}Bu)$_2$}MMe][B(C$_6$F$_5$)$_4$] ([**13a**]-[B(C$_6$F$_5$)$_4$], M = Al; [**13b**][B(C$_6$F$_5$)$_4$], M = Ga) and Ph$_3$CCH$_3$ (100% by ^{1}H NMR vs an internal standard, Scheme 6). The **13a**$^+$ and **13b**$^+$ cations decompose to unidentified species at 23 °C in C$_6$D$_5$Cl (**13a**$^+$, $t_{1/2} \approx$ 1 h; **13b**$^+$, $t_{1/2} \approx$ 7 h) and C$_6$D$_6$ (**13a**$^+$, $t_{1/2} \approx$ 2 h; **13b**$^+$, $t_{1/2} \approx$ 10 h), and thus [**13a**][B(C$_6$F$_5$)$_4$] and [**13b**][B(C$_6$F$_5$)$_4$] could not be isolated in pure form.

The ^{11}B, ^{19}F, and ^{13}C NMR spectra of [**13a**][B(C$_6$F$_5$)$_4$] and [**13b**][B(C$_6$F$_5$)$_4$] (C$_6$D$_5$Cl) establish that the B(C$_6$F$_5$)$_4^-$ anion is free in solution. The ^{1}H NMR spectra of **13a**$^+$ and **13b**$^+$ (C$_6$D$_5$-Cl) contain two ^{t}Bu signals in a 2/1 ratio and one M*Me* signal (**13a**$^+$, δ −0.04; **13b**$^+$, δ 0.35). The M*Me* resonances are shifted significantly downfield from the M*Me* resonances of **12a** and **12b** (δ −0.66; δ −0.17), which is consistent with more electron-deficient metal centers in **13a**$^+$ and **13b**$^+$ vs **12a** and **12b**. These data are consistent with base-free, three-coordinate **13a**$^+$ and **13b**$^+$ cations or solvated, four-coordinate **13a**$^+$·C$_6$D$_5$Cl and **13b**$^+$·C$_6$D$_5$Cl cations. For comparison, three-coordinate β-diketiminate {HC(CMeN(2,6-^{i}Pr$_2$-Ph))$_2$}AlR$^+$ complexes have been characterized crystallographically.[7b,c]

Chart 4
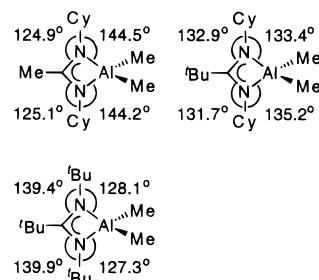
Attempts to generate the amine adduct [{^{t}BuC(N^{t}Bu)$_2$}Al-(Me)(NMe$_2$Ph)][B(C$_6$F$_5$)$_4$] by reaction of **13a**$^+$ with 1 equiv of NMe$_2$Ph or by reaction of **12a** with 1 equiv of [HNMe$_2$Ph]-[B(C$_6$F$_5$)$_4$] led to the formation of unidentified species. In contrast, the reaction of **13b**$^+$ with 1 equiv of NMe$_2$Ph in C$_6$D$_5$-Cl (10 min, 23 °C) yields the amine adduct [{^{t}BuC(N^{t}Bu)$_2$}-Ga(Me)(NMe$_2$Ph)][B(C$_6$F$_5$)$_4$] ([**14b**][B(C$_6$F$_5$)$_4$], 100% by ^{1}H NMR vs an internal standard, Scheme 6). [**14b**][B(C$_6$F$_5$)$_4$] is stable in C$_6$D$_5$Cl for several days at 23 °C, which contrasts with the apparent low stability of the Al analogue, which could not be observed. However, numerous attempts to isolate [**14b**]-[B(C$_6$F$_5$)$_4$] in pure form were unsuccessful due to its oily nature.

Discussion

Influence of Amidinate Steric Properties on the Structures of Cationic Al and Ga Complexes. Aluminum and gallium {RC(NR′)$_2$}MMe$_2$ complexes undergo methyl abstraction by the "cationic activators" [Ph$_3$C][B(C$_6$F$_5$)$_4$] and B(C$_6$F$_5$)$_3$ to yield cationic products. The stoichiometry of the reactions and the structures of the cations that are produced are determined primarily by the steric properties of the amidinate ligands. The acetamidinate complexes {MeC(NR′)$_2$}AlMe$_2$ (R′ = ^{i}Pr, **1a**; R′ = Cy, **3a**) react with 0.5 equiv of [Ph$_3$C][B(C$_6$F$_5$)$_4$] or B(C$_6$F$_5$)$_3$ to yield the double-amidinate-bridged dinuclear cations **2a**$^+$ and **4a**$^+$, in which the two metal centers are linked by μ-η^1,η^1 and μ-η^1,η^2 amidinate bridges. The Ga complex {MeC(N^{i}Pr)$_2$}-GaMe$_2$ (**1b**) reacts with 0.5 equiv of B(C$_6$F$_5$)$_3$ to yield the analogous dinuclear cationic Ga alkyl species **2b**$^+$. The bulkier ^{t}Bu-substituted amidinate complexes {^{t}BuC(N^{i}Pr)$_2$}MMe$_2$ (M = Al, **6a**; M = Ga, **6b**) react with 0.5 equiv of [Ph$_3$C][B(C$_6$F$_5$)$_4$] or B(C$_6$F$_5$)$_3$ to yield the single-amidinate-bridged dinuclear cations **7a**$^+$ and **7b**$^+$, in which the two metal centers are linked by a μ-η^1,η^2 amidinate. These dinuclear cations are presumed to form by initial generation of base-free {RC(NR′)$_2$}MMe$^+$ species and subsequent trapping by {RC(NR′)$_2$}MMe$_2$. In contrast, the "super-bulky" amidinate complexes {^{t}BuC(N^{t}Bu)$_2$}-MMe$_2$ (M = Al, **12a**; M = Ga, **12b**) react with 1 equiv of [Ph$_3$C][B(C$_6$F$_5$)$_4$] to yield {^{t}BuC(N^{t}Bu)$_2$}MMe$^+$ cations **13a**$^+$ and **13b**$^+$. The available data for **13a**$^+$ and **13b**$^+$ are consistent with base-free, three-coordinate structures or labile, four-coordinate solvated cations; however, these species decompose rapidly in solution to unidentified products, which hindered characterization.

Comparison of key bond angles in {RC(NR′)$_2$}AlMe$_2$ complexes as a function of the C-*R* and N-*R*′ substituents provides insight to the role of steric effects in the methyl abstraction reactions (Chart 4).[52] Replacement of the Me group at the central carbon of a {MeC(NR′)$_2$}AlMe$_2$ (R′ = ^{i}Pr, Cy)[53] complex by a ^{t}Bu group decreases the *R*′−N−Al angle by ca. 10°, to ca. 134°.

(52) The Ga analogues exhibit very similar structural trends.

(53) The steric bulk of the N-*Cy* substituent is very similar to that of the N-^{i}Pr substituent; see ref 17.
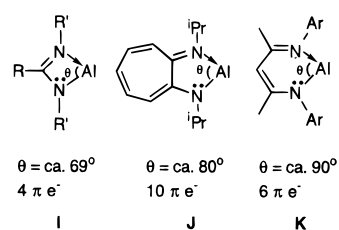
Chart 5

Chart 6
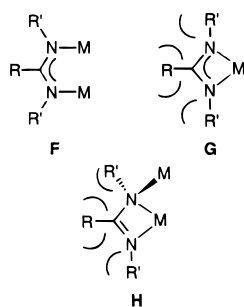
Similarly, replacement of the N-*Cy* (or N-*iPr*) substituents of a {*t*BuC(NR')$_2$}AlMe$_2$ (R' = *i*Pr, Cy) complex by a *t*Bu group decreases the R'−N−Al angle a further 7°, to ca. 127°. Thus, the degree of steric crowding at Al increases dramatically as *t*Bu substituents are incorporated into the amidinate ligand. The steric crowding at the metal centers in {*t*BuC(N*t*Bu)$_2$}MMe$^+$ and {*t*BuC(N*t*Bu)$_2$}MMe$_2$ prevents the formation of the corresponding dinuclear adduct.

The difference in the structures of the double-amidinate-bridged cations **2a$^+$**, **2b$^+$**, and **4a$^+$** and the single-amidinate-bridged cations **7a$^+$** and **7b$^+$** can also be traced to steric factors. As illustrated in Chart 5, in an idealized amidinate structure with 120° bond angles at the C and N centers, the nitrogen sp^2 donor orbitals project in parallel directions, which favors μ-η^1,η^1-bridged structures (**F**, Chart 5). However, increased steric interactions between the amidinate substituents will tend to decrease the N−C−N angle, which in turn will favor chelated or μ-η^1,η^2-bridged structures (**G** or **H**, Chart 5). For example, formamidinates and acetamidinates are well known to form transition metal complexes with μ-η^1,η^1-bridged structures of type **F**.[9a] There are also several examples of dinuclear group 13 complexes with μ-η^1,η^1 amidinate bridges, including [{μ-η^1,η^1-MeC(NMe)$_2$}$_2$MMe$_2$]$_2$ (M = Al, Ga)[20] and [{μ-η^1,η^1-HC(NCy)$_2$}$_2$InMe]$_2$.[54] In these cases, the amidinate ligands contain at least one sterically small substituent and the N−C−N angles are ca. 118°. In contrast, the bulkier systems {RC(NR')$_2$}MMe$_2$ (R = Me, *t*Bu; R' = *i*Pr, Cy, *t*Bu; M = Al, Ga) all adopt monomeric chelated amidinate structures with N−C−N angles of ca. 109°.[17,41] The μ-η^1,η^1 and μ-η^1,η^2 amidinate ligands in **2a$^+$** and **4a$^+$** are characterized by N−C−N angles of ca. 119° and 109°, respectively. In **4a$^+$**, the shortest H−H distance between the C*Me* and the *Cy* substituents of the μ-η^1,η^2 amidinate (N(1)−C(10)−N(2), Figure 1) is 2.24 Å, which is only slightly less than the sum of the van der Waals radii (ca. 2.4 Å). However, in the μ-η^1,η^1 amidinate of **4a$^+$**, much shorter C*Me*/*Cy* H−H contacts (1.88 Å) are observed, indicating that significant steric interactions between the C*Me* and *Cy* groups are present due to the larger N−C−N angle. As noted above, changing the C*R* group from Me to *t*Bu significantly increases the C*R*/NR' steric interactions, which apparently precludes formation of μ-η^1,η^1-bridged structures for **7a$^+$** and **7b$^+$**.

Bonding Trends in Dinuclear [{L−X}MR·{L−X}AlR$_2$]$^+$ Species. The μ-η^1,η^1 and μ-η^1,η^2 amidinate-bridged structures observed for the Al and Ga {RC(NR')$_2$}$_2$M$_2$Me$_3^+$ cations contrast with the Me-bridged structures observed for the analogous aminotroponiminate and diketiminate species {(ATI)-AlMe}$_2$(μ-Me)$^+$ and ({HC(CMeNAr)$_2$}AlMe)$_2$Me$^+$ (Ar = 2-*t*Bu-Ph).[4b,7c] In all three cases, the three-center, four-electron N-bridges are probably electronically favored over the two-center, two-electron methyl bridges. However, the acute N−Al−N

bite angle (ca. 69°; **I** in Chart 6) and compact size of the {RC-(NR')$_2$}Al unit facilitate the binding of two {RC(NR')$_2$}Al units to a single nitrogen center in the μ-η^1,η^2 amidinate-bridged structures. In contrast, the larger N−Al−N bite angles and concomitant increased crowding in the (ATI)Al (ca. 83°; **J** in Chart 6) and {HC(CMeNAr)$_2$}Al (ca. 96°; **K** in Chart 6) systems disfavor N-bridged structures.

It should also be noted that there are significant electronic differences between the amidinate and the ATI and diketiminate systems, as illustrated by the localized structures in Chart 6. The nitrogen lone pair in a RC(NR')$_2$}M unit is associated with a four-electron π-system, while those in (ATI)Al and {HC-(CMeNAr)$_2$}Al units are associated with ten- and six-electron π-systems, respectively. The increased π-delocalization and potential aromatic character in the latter systems may decrease the nucleophilicity of the N centers and disfavor N-bridged structures.

Al versus Ga. In several cases, parallel methyl abstraction chemistry is observed for Al and Ga amidinate compounds. The Al and Ga {MeC(N*i*Pr)$_2$}MMe$_2$ complexes **1a** and **1b** react with B(C$_6$F$_5$)$_3$ to yield **2a$^+$** and **2b$^+$**, and the Al and Ga {*t*BuC-(NR')$_2$}MMe$_2$ (R' = *i*Pr, *t*Bu) complexes react with B(C$_6$F$_5$)$_3$ and [Ph$_3$C][B(C$_6$F$_5$)$_4$] to yield the analogous pairs of complexes **7a$^+$** and **7b$^+$**, and **13a$^+$** and **13b$^+$**. In contrast, while the Al complexes {RC(N*i*Pr)$_2$}AlMe$_2$ (**1a**, R = Me; **6a**, R = *t*Bu) react with [HNMe$_2$Ph][B(C$_6$F$_5$)$_4$] to yield the cationic amine adducts **5a$^+$** and **8a$^+$** and methane, the Ga analogues **1b** and **6b** do not undergo Ga−Me protonolysis by this reagent. Additionally, while **1a** cleanly reacts with [Ph$_3$C][B(C$_6$F$_5$)$_4$] to yield **2a$^+$**, the Ga analogue **1b** does not undergo Me$^-$ abstraction by Ph$_3$C$^+$. These reactivity differences are ascribed to the lower polarity of the Ga−Me bonds vs the Al−Me bonds in these systems. The acid HNMe$_2$Ph$^+$ apparently reacts with the amidinate ligands of **1b** and **6b**, although the products of these reactions have not been identified. Similarly, the Ph$_3$C$^+$ ion may attack the amidinate ligand of **1b** rather that the Ga−Me bond; however, steric crowding in the *t*Bu-substituted analogue **6b** directs the attack of Ph$_3$C$^+$ to a Ga−Me bond. As initially anticipated, the Ga cations (**2b$^+$**, **7b$^+$**, and **13b$^+$**) are more stable than their Al counterparts (**2a$^+$**, **7a$^+$**, and **13a$^+$**), which was of significant assistance in characterization of the latter systems.

Dynamic and Reactivity Properties of 2a$^+$ and 7a$^+$. The dynamic and reactivity properties of the two types of dinuclear Al cations, i.e., **2a$^+$** vs **7a$^+$**, are very different. The double-amidinate-bridged dinuclear cation **2a$^+$** undergoes two different fluxional processes: μ-η^1,η^1/μ-η^1,η^2 amidinate exchange (process (i)) and Al-*Me* exchange between the two Al centers (process (ii)), while **7a$^+$** is nonfluxional up to 60 °C. However, intermolecular exchange is not observed between **2a$^+$** and **1a**, nor between **7a$^+$** and **6a**, which shows that neither dinuclear cation dissociates to mononuclear species easily. The dinuclear cations are cleaved by Lewis bases and thus are potential source of {RC(N*i*Pr)$_2$}AlMe$^+$ or {RC(N*i*Pr)$_2$}AlMe(L)$^+$ species, but the double-amidinate-bridged **2a$^+$** is significantly less reactive than the single-amidinate-bridged **7a$^+$**. Thus, **2a$^+$** slowly reacts

(54) Zhou, Y.; Richeson, D. S. *Inorg. Chem.* **1996**, *35*, 1423.

Cationic Al and Ga Amidinate Complexes

J. Am. Chem. Soc., Vol. 122, No. 2, 2000 285

with 1 equiv of NMe₂Ph (12 h, 23 °C) to yield a 1/1 mixture of the amine adduct **5a⁺** and **1a**, while **7a⁺** reacts very rapidly with NMe₂Ph (<10 min at 23 °C) to yield the corresponding amine adduct and the neutral precursor. The higher reactivity of **7a⁺** vs **2a⁺** toward cleavage to mononuclear species may contribute to the higher activity of **7a⁺** vs **2a⁺** in ethylene polymerization, although further investigation of this issue is required.[4a]

Importance of the Anion. As for cationic transition metal alkyl species, the stability of the cationic Al and Ga amidinate alkyl species is strongly influenced by the counterion properties. Compounds [**7a**][B(C₆F₅)₄] and [**7b**][B(C₆F₅)₄] are more stable in solution than [**7a**][MeB(C₆F₅)₃] and [**7b**][MeB(C₆F₅)₃], due to the C₆F₅⁻ transfer in the latter salts. The choice of an appropriate anion is critical for cation stability in these systems, and thus is important for potential application of these cations.

Conclusions

Aluminum and gallium {RC(NR′)₂}MMe₂ complexes react with "cationic activators" to yield cationic alkyl species whose structures are strongly influenced by the steric properties of the amidinate ligand. Three types of structure are observed: (i) fluxional double-amidinate-bridged dinuclear species {RC-(NR′)₂}₂M₂Me₃⁺ containing μ-η^1,η^1 and μ-η^1,η^2 amidinates, (ii) rigid single-amidinate-bridged dinuclear species {RC(NR′)₂}-MMe·{RC(NR′)₂}MMe₂⁺ containing a μ-η^1,η^2 amidinate, and (iii) thermally unstable base-free (three-coordinate) or solvated (four-coordinate) "{RC(NR′)₂}MMe⁺" species. The preference for amidinate-bridged structures contrasts with preference for the Me-bridged structures observed for the {(ATI)AlMe}₂(μ-Me)⁺ and ({HC(CMeNAr)₂}AlMe)₂Me⁺ (Ar = 2-ᵗBu-Ph) systems. The results reported here provide a starting point for understanding the mechanism and reactivity trends in ethylene polymerization catalyzed by cationic Al species. Studies concerning the influence of the amidinate electronic properties and the nature of the Al-*R* group on the structures and reactivity of cationic Al amidinate species will be reported in due course.

Experimental Section

General Procedures. All experiments were carried out under N₂ using standard Schlenk techniques or in a Vacuum Atmospheres glovebox. Benzene, toluene, pentane, hexanes, and diethyl ether were distilled from Na/benzophenone and stored under N₂ prior to use. CH₂Cl₂, CD₂Cl₂, ClCD₂CD₂Cl, and C₆D₅Cl were distilled from CaH₂ and stored under vacuum prior to use. The Al and Ga amidinate dimethyl complexes **1a**, **3a**, **6a**, **10a**, **1b**, **6b**, and **12b** were prepared by salt metathesis procedures.[17,41] [Ph₃C][B(C₆F₅)₄] was prepared by a literature procedure.[55,56] [NHMe₂Ph][B(C₆F₅)₄] and B(C₆F₅)₃ were obtained as a gift from Boulder Scientific.[57] All other chemicals were purchased from Aldrich and used as received, except NMe₂Ph which was dried over molecular sieves (4 Å) prior to use.

¹H, ¹³C, and ¹¹B NMR spectra were obtained on a Bruker AMX-360 spectrometer, in Teflon-valved or flame-sealed tubes, at ambient probe temperature (23 °C) unless otherwise indicated. ¹⁹F NMR spectra were obtained on a Bruker AC-300 spectrometer. ¹H and ¹³C NMR chemical shifts are reported vs SiMe₄ and were determined by reference to the residual solvent peaks. The residual ¹H NMR resonances for C₆D₅Cl appear at δ 7.14, 7.00, and 6.96, and the ¹³C NMR resonances

(55) (a) Chien, J. C. W.; Tsai, W. M.; Rausch, M. D. *J. Am. Chem. Soc.* **1991**, *113*, 8570. (b) See also ref 4b.

(56) Data for [Ph₃C][B(C₆F₅)₄]. ¹H NMR (C₆D₅Cl): δ 7.68 (t, *J* = 7.2, 3H, *p*-Ph), 7.31 (t, *J* = 7.6, 6H, *m*-Ph), 7.08 (d, *J* = 7.2, 6H, *o*-Ph). ¹¹B NMR (C₆D₅Cl): δ −16.5 (br s). ¹⁹F NMR (C₆D₅Cl): δ −132.5 (m, 8F, *o*-C₆F₅), −163.2 (t, ³*J*_FF = 20, 4F, *p*-C₆F₅), −167.0 (br s, 8F, *m*-C₆F₅).

(57) Data for B(C₆F₅)₃. ¹⁹F NMR (C₆D₅Cl): δ −128.4 (br, 6F, *o*-C₆F₅), −143.2 (br, 3F, *p*-C₆F₅), −160.6 (br, 6F, *m*-C₆F₅). ¹¹B NMR (C₆D₅Cl, 80 °C): δ 61 (br).

for C₆D₅Cl appear at δ 134.2, 129.3 (t), 128.3(t), and 126.0(t). ¹¹B NMR chemical shifts are reported vs BF₃·Et₂O (0.1 M in C₆D₅Cl). ¹⁹F NMR chemical shifts are reported vs CFCl₃ in CDCl₃. All coupling constants are reported in hertz. Mass spectra were obtained using the direct insertion probe (DIP) method on a VG Analytical Trio I instrument operating at 70 eV. Elemental analyses were performed by Desert Analytics Laboratory (Tucson, AZ).

[{MeC(NⁱPr)₂}₂Al₂Me₃][MeB(C₆F₅)₃] ([2a][MeB(C₆F₅)₃]). A solution of B(C₆F₅)₃ (770 mg, 1.50 mmol) in CH₂Cl₂ (20 mL) was added to {MeC(NⁱPr)₂}AlMe₂ (**1a**, 600 mg, 3.00 mmol). The reaction mixture was stirred for 30 min at 23 °C, and the volatiles were removed under vacuum, leaving a colorless oily residue. Trituration with pentane afforded pure [**2a**][MeB(C₆F₅)₃] as a white solid (910 mg, 83%). ¹H NMR (CD₂Cl₂, 23 °C): δ 3.79 (sept, ³*J* = 6.6, 4H, C*H*Me₂), 2.31 (s, 6H, C*Me*), 1.28 (d, ³*J* = 6.5, CH*Me*₂), 0.48 (br s, 3H, *Me*B), −0.38 (br s, 9H, Al*Me*). ¹H NMR (CD₂Cl₂, −20 °C): δ 3.75 (br sept, ³*J* = 5.9, 4H, C*H*Me₂), 2.28 (s, 6H, C*Me*), 1.24 (br s, 24H, CH*Me*₂), 0.52 (br s, 3H, *Me*B), −0.15 (br s, 3H, Al*Me*), −0.57 (br s, 6H, Al*Me*). ¹H NMR (CD₂Cl₂, −85 °C): δ 3.79 (br sept, 1H, C*H*Me₂), 3.67 (br sept, 3H, C*H*Me₂), 2.33 (s, 3H, C*Me*), 2.15 (s, 3H, C*Me*), 1.30 (m, 9H, CH*Me*₂), 1.18 (m, 6H, CH*Me*₂), 1.02 (m, 9H, CH*Me*₂), 0.55 (br s, 3H, *Me*B), −0.17 (br s, 3H, Al*Me*), −0.54 (br s, 3H, Al*Me*), −0.75 (s, 3H, Al*Me*). ¹³C NMR (CD₂Cl₂, 23 °C): δ 182.0 (*C*Me), 148.6 (d, ¹*J*_CF = 235, *C*₆F₅), 137.9 (d, ¹*J*_CF = 243, *C*₆F₅), 136.8 (d, ¹*J*_CF = 246, *C*₆F₅), 129.7 (br s, *ipso*-*C*₆F₅), 50.5 (d, ¹*J*_CH = 139, *C*HMe₂), 23.4 (q, ¹*J*_CH = 127, CH*Me*₂), 17.8 (q, ¹*J*_CH = 130, C*Me*), 9.2 (*Me*B), −5.6 (br q, ¹*J*_CH = 114, Al*Me*). ¹³C NMR (CD₂Cl₂, −85 °C): δ 182.4 (Me*C*), 179.4 (Me*C*), 148.7 (d, ¹*J*_CF = 238, *C*₆F₅), 137.8 (d, ¹*J*_CF = 242, *C*₆F₅), 135.3 (d, ¹*J*_CF = 236, *C*₆F₅), 130.5 (br s, *ipso*-*C*₆F₅), 50.3 (*C*HMe₂), 50.1 (*C*HMe₂), 49.5 (*C*HMe₂), 48.8 (*C*HMe₂), 23.4 (CH*Me*₂), 22.9 (CH*Me*₂), 22.8 (CH*Me*₂), 22.6 (CH*Me*₂), 22.2 (CH*Me*₂), 22.0 (CH*Me*₂), 21.8 (CH*Me*₂), 21.6 (CH*Me*₂), 16.6 (*Me*C), 14.1 (*Me*C), 9.4 (*Me*B), −3.8 (Al*Me*), −6.6 (Al*Me*), −6.6 (Al*Me*). ¹¹B NMR (CD₂Cl₂, 23 °C): δ −14 (br). ¹⁹F NMR (CD₂Cl₂): δ −131.6 (6F, *o*-C₆F₅), −163.6 (3F, *p*-C₆F₅), 166.3 (6F, *m*-C₆F₅). Anal. Calcd for C₃₈H₄₆Al₂BF₁₅N₄: C, 50.23; H, 5.10; N, 6.17. Found: C, 50.46; H, 4.92; N, 6.09.

[{MeC(NⁱPr)₂}₂Al₂Me₃][B(C₆F₅)₄] ([2a][B(C₆F₅)₄]). A solution of [Ph₃C][B(C₆F₅)₄] (402 mg, 0.436 mmol) in CH₂Cl₂ (5 mL) was cannula-transferred at 23 °C to {MeC(NⁱPr)₂}AlMe₂ (**1a**, 173 mg, 0.872 mmol), and the mixture was stirred for 30 min. The volatiles were removed under vacuum, leaving a colorless oily residue. The residue was triturated with pentane to afford a white solid. The mixture was filtered through a glass frit, and the solid was washed with pentane (3 × 5 mL) and dried under vacuum, affording pure [**2a**][B(C₆F₅)₄] (324 mg, 78%). The NMR spectra of [**2a**][B(C₆F₅)₄] exhibit resonances for **2a⁺** that are identical to those for [**2a**][MeB(C₆F₅)₃] (see above) and resonances for the B(C₆F₅)₄⁻ anion that are listed here. ¹³C NMR (C₆D₅Cl):[58] δ 149.0 (d, ¹*J*_CF = 241, *C*₆F₅), 138.8 (d, ¹*J*_CF = 245, *C*₆F₅), 136.9 (d, ¹*J*_CF = 243, *C*₆F₅). ¹¹B NMR (C₆D₅Cl): δ −16.5 (br s). ¹⁹F NMR (C₆D₅Cl): δ −132.5 (m, 8F, *o*-C₆F₅), −163.2 (t, ³*J*_FF = 20, 4F, *p*-C₆F₅), −167.0 (br s, 8F, *m*-C₆F₅). Anal. Calcd for C₄₃H₄₃Al₂BF₂₀N₄: C, 48.69; H, 4.09; N, 5.28. Found: C, 48.91; H, 4.22; N, 5.19.

[{MeC(NⁱPr)₂}₂Ga₂Me₃][MeB(C₆F₅)₃] ([2b][MeB(C₆F₅)₃]). A CH₂Cl₂ solution (1 mL) of {MeC(NⁱPr)₂GaMe₂ (**1b**, 236 mg, 0.98 mmol) was added by cannula to a hexane solution (15 mL) of B(C₆F₅)₃ (250 mg, 0.490 mmol). The reaction mixture was stirred for 3 h at 23 °C, resulting in a white suspension. The mixture was filtered through a glass frit. The colorless solid was washed with hexane (3 × 5 mL) and dried under vacuum to afford pure [**2b**][MeB(C₆F₅)₃] as a colorless solid in 71% yield. ¹H NMR (C₆D₅Cl): δ 3.25 (br, 4H, C*H*Me₂), 1.69 (s, 6H, *Me*C), 1.03 (br s, 3H, *Me*B), 0.78 (br, 24H, CH*Me*₂), 0.12 (br, 3H, Ga*Me*), −0.32 (br, 6H, Ga*Me*). ¹H NMR (C₆D₅Cl, 60 °C): δ 3.36 (sept, ³*J* = 6.5, 4H, C*H*Me₂), 1.77 (s, 6H, *Me*C), 0.98 (br s, 3H, *Me*B), 0.87 (d, 24H, ³*J* = 6.1, CH*Me*₂), −0.14 (br, 9H, Ga*Me*). ¹H NMR (CD₂Cl₂, −85 °C): δ 3.71 (br, 3H, C*H*Me₂), 3.55 (br, 1H, C*H*Me₂), 2.14 (s, 3H, *Me*C), 2.10 (s, 3H, *Me*C), 1.25 (br, 6H, CH*Me*₂), 1.11 (br, 9H, CH*Me*₂), 0.98 (br, 6H, CH*Me*₂), 0.92 (br, 3H, CH*Me*₂), 0.55 (br, 3H, *Me*B), 0.43 (s, 3H, Ga*Me*), −0.04 (s, 3H, Ga*Me*), −0.27 (s, 3H, Ga*Me*).

(58) The *ipso*-B(C₆F₅)₄⁻ resonance was obscured by the solvent resonances.

^{13}C NMR (C$_6$D$_5$Cl, 23 °C):^{59} δ 179.7 (MeC), 150.1 (d, $^1J_{CF}$ = 238, C_6F_5), 139.2 (d, $^1J_{CF}$ = 242, C_6F_5), 136.7 (d, $^1J_{CF}$ = 236, C_6F_5), 51.5 (CHMe$_2$), 24.0 (CHMe_2), 17.3 (MeC), 11.3 (MeB), 0.4 (GaMe), 0.4 (GaMe). ^{13}C NMR (CD$_2$Cl$_2$, −85 °C): δ 179.8 (MeC), 176.0 (MeC), 148.7 (d, $^1J_{CF}$ = 238, C_6F_5), 137.8 (d, $^1J_{CF}$ = 242, C_6F_5), 135.3 (d, $^1J_{CF}$ = 236, C_6F_5), 128.7 (br s, ipso-C_6F_5), 50.6 (CHMe$_2$), 50.4 (CHMe$_2$), 49.3 (CHMe$_2$), 48.6 (CHMe$_2$), 24.5 (CHMe_2), 23.2 (CHMe_2), 22.9 (CHMe_2), 22.7 (CHMe_2), 22.2 (CHMe_2), 22.0 (CHMe_2), 21.5 (CHMe_2), 16.8 (MeC), 15.4 (MeC), 9.4 (MeB), 0.9 (GaMe), −0.75 (GaMe), −3.1 (GaMe). ^{11}B NMR (C$_6$D$_5$Cl): δ −14 (br s). ^{19}F NMR (C$_6$D$_5$Cl): δ −131.9 (m, 6F, o-C_6F_5), −164.7 (t, $^3J_{FF}$ = 20, 3F, p-C_6F_5), −167.3 (m, 6F, m-C_6F_5). Anal. Calcd for C$_{38}$H$_{46}$BF$_{15}$Ga$_2$N$_4$: C, 45.90; H, 4.67; N, 5.64. Found: C, 46.13; H, 4.86; N, 5.23.

[{MeC(NCy)$_2$}$_2$Al$_2$Me$_3$][B(C$_6$F$_5$)$_4$] ([4a][B(C$_6$F$_5$)$_4$]). A slurry of {MeC(NCy)$_2$}AlMe$_2$ (**3a**, 200 mg, 0.720 mmol) and 0.5 equiv of [Ph$_3$C]-[B(C$_6$F$_5$)$_4$] (331 mg, 0.359 mmol) in hexane (5 mL) was vigorously stirred at 23 °C for 3 d, yielding a colorless slurry. The mixture was filtered through a glass frit, and the colorless solid was washed several times with pentane and dried under vacuum to afford [4a][B(C$_6$F$_5$)$_4$] as a colorless solid in 61% yield. ^{1}H NMR (C$_6$D$_5$Cl): δ 3.10 (br, 4H, NCH)), 1.92 (s, 6H, CMe), 1.80−1.45 (br, 16H, Cy), 1.40−0.80 (br, 24H, Cy), −0.43 (br s, 9H, AlMe). Anal. Calcd for C$_{55}$H$_{59}$Al$_2$BF$_{20}$N$_4$: C, 54.10; H, 4.88; N, 4.59. Found: C, 54.46; H, 4.92; N, 4.71.

Generation of [{MeC(N^{i}Pr)$_2$}Al(Me)(NMe$_2$Ph)][B(C$_6$F$_5$)$_4$] ([5a]-[B(C$_6$F$_5$)$_4$]). A solution of [HNMe$_2$Ph][B(C$_6$F$_5$)$_4$] (853 mg, 0.106 mmol) in CD$_2$Cl$_2$ (5 mL) was added to a vial containing {MeC(N^{i}Pr)$_2$}AlMe$_2$ (**1a**, 211 mg, 106 mmol). The resulting solution was transferred to an NMR tube and maintained at 23 °C for 15 min. NMR spectra were recorded and indicated that 100% conversion to [5a][B(C$_6$F$_5$)$_4$] had occurred. ^{1}H NMR (CD$_2$Cl$_2$): δ 7.63 (t, ^3J = 7.9, 2H, m-Ph), 7.51 (t, ^3J = 7.3, 1H, p-Ph), 7.47 (d, ^3J = 7.9, 2H, o-Ph), 3.58 (sept, ^3J = 6.4, 2H, CHMe$_2$), 3.20 (s, 6H, NMe$_2$Ph), 2.17 (s, 3H, CMe), 1.03 (d, ^3J = 6.5, 6H, CHMe_2), 0.92 (d, ^3J = 6.4, 6H, CHMe_2), −0.30 (s, 3H, AlMe). ^{13}C NMR (CD$_2$Cl$_2$): δ 182.0 (CMe), 148.6 (d, $^1J_{CF}$ = 245, C_6F_5), 143.7 (ipso-NMe$_2$$Ph$), 138.6 (d, $^1J_{CF}$ = 245, C_6F_5), 136.7 (d, $^1J_{CF}$ = 243, C_6F_5), 131.4 (NMe$_2$$Ph$), 129.8 (NMe$_2$$Ph$), 125.1 (br, ipso-$C_6F_5$), 120.9 (NMe$_2$$Ph$), 46.7 (N$Me_2$Ph), 46.0 (CHMe$_2$), 24.7 (CH$Me_2$), 24.6 (CH$Me_2$), 12.7 (C$Me$), −13.4 (br, Al$Me$).

Generation of [{MeC(N^{i}Pr)$_2$}Al(Me)(NMe$_2$Ph)][MeB(C$_6$F$_5$)$_3$] ([5a][MeB(C$_6$F$_5$)$_3$]). NMe$_2$Ph (7.3 mg, 0.032 mmol) was added to a solution of [({MeC(N^{i}Pr)$_2$}Al)$_2$Me$_3$][MeB(C$_6$F$_5$)$_3$] ([2a][MeB(C$_6$F$_5$)$_3$], 27.0 mg, 0.032 mmol) in CD$_2$Cl$_2$ (0.6 mL). The mixture was stirred for 15 min and transferred to an NMR tube. The tube was maintained at 23 °C, and the reaction was monitored by ^{1}H NMR. The NMR spectra showed that complete conversion to a 1/1 mixture of [5a][MeB(C$_6$F$_5$)$_3$] and {MeC(N^{i}Pr)$_2$}AlMe$_2$ had occurred after 12 h. The NMR spectra for [5a][MeB(C$_6$F$_5$)$_3$] are identical to those for [5a][B(C$_6$F$_5$)$_4$], except for the MeB(C$_6$F$_5$)$_3$$^-$ resonances which are listed here. ^{1}H NMR (CD$_2$-Cl$_2$): δ 0.48 (br s, 3H, MeB). ^{13}C NMR (CD$_2$Cl$_2$): δ 148.6 (d, $^1J_{CF}$ = 235, C_6F_5), 137.9 (d, $^1J_{CF}$ = 243, C_6F_5), 136.8 (d, $^1J_{CF}$ = 246, C_6F_5), 129.7 (br s, ipso-C_6F_5). ^{11}B NMR (CD$_2$Cl$_2$): δ −14 (br).

Generation of [{^{t}BuC(N^{i}Pr)$_2$}AlMe$_2$·{^{t}BuC(N^{i}Pr)$_2$}AlMe][B(C$_6$F$_5$)$_4$] ([7a][B(C$_6$F$_5$)$_4$]). An NMR tube was charged with {^{t}BuC(N^{i}Pr)$_2$}AlMe$_2$ (**6a**, 21.2 mg, 0.0820 mmol) and [Ph$_3$C][B(C$_6$F$_5$)$_4$] (40.7 mg, 0.0410 mmol), and C$_6$D$_5$Cl (0.5 mL) was added by vacuum transfer at −78 °C. The tube was flame-sealed under vacuum, warmed to 23 °C, and vigorously shaken. A pale brown solution formed, and the tube was maintained at 23 °C for 15 min. A ^{1}H NMR spectrum was recorded at 25 °C, showing that a 1/1 mixture of Ph$_3$CCH$_3$ and [7a][B(C$_6$F$_5$)$_4$] had formed. Numerous attempts to isolate [7a][B(C$_6$F$_5$)$_4$] in pure form were unsuccessful due to the thermal instability of this species.

Data for Ph$_3$CCH$_3$. ^{1}H NMR (C$_6$D$_5$Cl): δ 7.15−7.00 (m, 15H, Ph), 2.03 (s, 3H, CH_3). ^{13}C NMR (C$_6$D$_5$Cl): δ 150.1 (ipso-Ph), 129.0 (Ph), 128.0 (Ph), 126.1 (Ph), 52.6 (CCH$_3$), 30.6 (CH$_3$).

Data for [7a][B(C$_6$F$_5$)$_4$]. ^{1}H NMR (C$_6$D$_5$Cl): δ 4.05−3.75 (m, 4H, CHMe$_2$), 1.15 (s, 9H, CMe_3), 1.14 (s, 9H, CMe_3), 1.00−0.89 (m, 24H, CHMe_2), −0.36 (s, 3H, AlMe), −0.39 (s, 3H, AlMe), −0.42 (s, 3H, AlMe). ^{13}C NMR (CD$_2$Cl$_2$, −85 °C): δ 188.2 (CCMe$_3$), 187.6 (CCMe$_3$),

149.1 (d, $^1J_{CF}$ = 245, C_6F_5), 136.6 (d, $^1J_{CF}$ = 245, C_6F_5), 135.3 (d, $^1J_{CF}$ = 243, C_6F_5), 126.4 (br, ipso-C_6F_5), 46.7 (CHMe$_2$), 45.7 (CHMe$_2$), 45.3 (CHMe$_2$), 45.0 (CHMe$_2$), 41.5 (CCMe$_3$), 40.0 (CCMe$_3$), 28.1 (CCMe_3), 28.0 (CCMe_3), 25.8 (CHMe_2), 25.6 (CHMe_2), 25.5 (CHMe_2), 24.4 (CHMe_2), 23.5 (CHMe_2), 22.6 (CHMe_2), 21.8 (CHMe_2), 21.7 (CHMe_2), −3.1 (AlMe), −3.5 (AlMe), −4.0 (AlMe). ^{11}B NMR (C$_6$D$_5$-Cl): δ −16.5 (br s). ^{19}F NMR (C$_6$D$_5$Cl): δ −132.5 (m, 8F, o-C_6F_5), −163.2 (t, $^3J_{FF}$ = 20, 4F, p-C_6F_5), −167.0 (br, 8F, m-C_6F_5).

Generation of [7a][MeB(C$_6$F$_5$)$_3$] from 6a and B(C$_6$F$_5$)$_3$ at −60 °C. An NMR tube was charged with {^{t}BuC(N^{i}Pr)$_2$}AlMe$_2$ (**6a**, 30.0 mg, 0.0125 mmol) and B(C$_6$F$_5$)$_3$ (63.9 mg, 0.0125 mmol), and CD$_2$Cl$_2$ (0.5 mL) was added by vacuum transfer at −78 °C. The tube was immersed in an acetone/dry ice bath (−78 °C) and was flame-sealed under vacuum at this temperature. The tube was removed from the −78 °C bath and vigorously shaken for 30 s, yielding a colorless solution, and was immediately inserted into the NMR probe which had been precooled at −60 °C. The probe was maintained at −60 °C for 20 min. A ^{1}H NMR spectrum was then recorded which showed that [7a][MeB(C$_6$F$_5$)$_3$] had formed in 80% yield. The ^{1}H and ^{13}C NMR data of [7a][MeB(C$_6$F$_5$)$_3$] are identical to those of [7a][B(C$_6$F$_5$)$_4$] except for the MeB(C$_6$F$_5$)$_3$$^-$ resonances, which are listed here.

Data for MeB(C$_6$F$_5$)$_3$$^-$. ^{1}H NMR (CD$_2Cl_2$, −60 °C): δ 0.57 (br s, MeB). ^{13}C NMR (CD$_2$Cl$_2$, −60 °C): δ 147.7 (d, $^1J_{CF}$ = 238, C_6F_5), 136.5 (d, $^1J_{CF}$ = 242, C_6F_5), 135.8 (d, $^1J_{CF}$ = 236, C_6F_5), 126.4 (br s, ipso-C_6F_5), 15.3 (q, $^1J_{CH}$ = 129, MeB). ^{11}B NMR (CD$_2$Cl$_2$, −60 °C): δ −14 (br s).

[{^{t}BuC(N^{i}Pr)$_2$}GaMe$_2$·{^{t}BuC(N^{i}Pr)$_2$}GaMe][B(C$_6$-F$_5$)$_4$] ([7b][B(C$_6$F$_5$)$_4$]). A mixture of {^{t}BuC(N^{i}Pr)$_2$}GaMe$_2$ (**6b**, 200 mg, 0.706 mmol) and [Ph$_3$C][B(C$_6$F$_5$)$_4$] (326 mg, 0.353 mmol) in benzene (1 mL) was stirred for 1 h at 23 °C. Hexane (10 mL) was added, resulting in the formation of two layers (deep red bottom layer and yellow top layer). The mixture was stirred at 23 °C for 2 d, resulting in the formation of a yellow solid. The mixture was filtered, and the solid was washed with pentane (3 × 5 mL) and dried under vacuum to afford pure [7b]-[B(C$_6$F$_5$)$_4$] (361 mg, 64%). ^{1}H NMR (CD$_2$Cl$_2$, −60 °C): δ 4.75 (septet, ^3J = 6.1, 1H, CHMe$_2$), 4.59 (septet, ^3J = 6.5, 1H, CHMe$_2$), 4.53−4.42 (m, 2H, CHMe$_2$), 1.73 (s, 9H, CMe_3), 1.65 (s, 9H, CMe_3), 1.68−1.27 (m, 24H, CHMe_2), 0.55 (s, 3H, GaMe), 0.45 (s, 3H, GaMe), 0.35 (s, 3H, GaMe). ^{13}C NMR (C$_6$D$_5$Cl): δ 186.7 (CCMe$_3$), 184.4 (CCMe$_3$), 149.0 (d, $^1J_{CF}$ = 241, C_6F_5), 138.8 (d, $^1J_{CF}$ = 245, C_6F_5), 136.9 (d, $^1J_{CF}$ = 243, C_6F_5), 52.3 (CHMe$_2$), 51.9 (CHMe$_2$), 47.7 (CHMe$_2$), 46.9 (CHMe$_2$), 41.2 (CCMe$_3$), 39.4 (CCMe$_3$), 29.1 (CCMe_3), 28.8 (CCMe_3), 27.4 (CHMe_2), 26.4 (CHMe_2), 26.0 (CHMe_2), 25.7 (CHMe_2), 24.6 (CHMe_2), 23.6 (CHMe_2), 23.2 (CHMe_2), 22.1 (CHMe_2), 3.6 (q, $^1J_{CH}$ = 125, GaMe), 1.3 (q, $^1J_{CH}$ = 123, GaMe), 1.3 (q, $^1J_{CH}$ = 123, GaMe). ^{11}B NMR (C$_6$D$_5$Cl): δ −16.5 (br s). ^{19}F NMR (C$_6$D$_5$Cl): δ −132.5 (m, 8F, o-C_6F_5), −163.2 (t, $^3J_{FF}$ = 20, 4F, p-C_6F_5), −167.0 (br, 8F, m-C_6F_5). Anal. Calcd for C$_{49}$H$_{55}$BF$_{20}$GaN$_2$: C, 47.83; H, 4.51; N, 2.28. Found: C, 48.24; H, 4.37; N, 2.13.

Generation of [{^{t}BuC(N^{i}Pr)$_2$}Al(Me)(NMe$_2$Ph)][B(C$_6$F$_5$)$_4$] ([8a]-[B(C$_6$F$_5$)$_4$]). (a) From [7a][B(C$_6$F$_5$)$_4$]. [{^{t}BuC(N^{i}Pr)$_2$}AlMe$_2$·{^{t}BuC-(N^{i}Pr)$_2$}AlMe][B(C$_6$F$_5$)$_4$] ([7a][B(C$_6$F$_5$)$_4$]) was generated in situ in C$_6$D$_5$Cl in a valved NMR tube as described above, and 1 equiv of NMe$_2$-Ph (10.3 μL, 0.0883 mmol) was added at 23 °C by syringe. The tube was vigorously shaken and maintained at 23 °C for 10 min. NMR spectra were then recorded and showed that complete conversion to a 1/1 mixture of [7a][B(C$_6$F$_5$)$_4$] and **6a** had occurred.

(b) From 6a. [8a][B(C$_6$F$_5$)$_4$] was generated by the procedure outlined above for [{MeC(N^{i}Pr)$_2$}Al(Me)(NMe$_2$Ph)][B(C$_6$F$_5$)$_4$] ([5a][B(C$_6$F$_5$)$_4$]), using 208 mg (0.0865 mmol) of {^{t}BuC(N^{i}Pr)$_2$}AlMe$_2$ (**6a**) and 694 mg (0.0866 mmol) of [HNMe$_2$Ph][B(C$_6$F$_5$)$_4$]. Quantitative conversion to [8a][B(C$_6$F$_5$)$_4$] was observed by ^{1}H and ^{13}C NMR. ^{1}H NMR (CD$_2$-Cl$_2$): δ 7.61−7.48 (m, 5H, NPh), 4.13 (sept, ^3J = 6.3, 2H, CHMe$_2$), 3.21 (s, 6H, NMe_2Ph), 1.42 (s, 3H, CMe_3), 1.00 (d, ^3J = 6.2, 6H, CHMe_2), 0.89 (d, ^3J = 6.3, 6H, CHMe_2), −0.11 (s, 3H, AlMe). ^{13}C NMR (CD$_2$Cl$_2$): δ 189.3 (CMe_3), 148.6 (d, $^1J_{CF}$ = 245, C_6F_5), 144.4 (ipso-NMe$_2$$Ph$), 138.6 (d, $^1J_{CF}$ = 245, C_6F_5), 136.7 (d, $^1J_{CF}$ = 243, C_6F_5), 131.2 (NMe$_2$$Ph$), 129.8 (NMe$_2$$Ph$), 125.1 (br, ipso-$C_6F_5$), 121.1 (NMe$_2$$Ph$), 47.1 (N$Me_2$Ph), 46.5 (CHMe$_2$), 29.3 (C$Me_3$), 26.9 (CH$Me_2$), 25.5 (CH$Me_2$), 12.7 (C$Me$), −10.9 (br, Al$Me$). ^{11}B NMR (C$_6D_5$Cl): δ

Table 1. Selected Bond Lengths (Å) and Angles (deg) for [{MeC(NCy)$_2$}$_2$Al$_2$Me$_3$][B(C$_6$F$_5$)$_4$] ([**4a**][B(C$_6$F$_5$)$_4$])

Al(1)−N(1)	2.027(1)	Al(2)−N(1)	1.979(1)
Al(1)−N(4)	1.959(1)	Al(2)−N(2)	1.927(1)
Al(1)−C(1)	1.949(2)	Al(2)−N(3)	1.866(2)
Al(1)−C(2)	1.971(2)	Al(2)−C(3)	1.942(2)
N(4)−C(24)	1.332(2)	N(1)−C(10)	1.435(1)
N(3)−C(24)	1.360(2)	N(2)−C(10)	1.289(2)
N(1)−Al(1)−N(4)	98.11(6)	N(2)−Al(2)−N(1)	69.51(6)
N(4)−Al(1)−C(1)	105.33(7)	N(1)−Al(2)−N(3)	109.30(6)
N(4)−Al(1)−C(2)	119.80(7)	N(1)−Al(2)−C(3)	119.52(7)
N(1)−Al(1)−C(1)	116.81(7)	N(2)−Al(2)−N(3)	108.64(6)
N(1)−Al(1)−C(2)	103.49(7)	N(2)−Al(2)−C(3)	114.32(7)
C(1)−Al(1)−C(2)	112.97(8)	N(3)−Al(2)−C(3)	123.06(7)
N(4)−C(24)−N(3)	119.0(2)	N(1)−C(10)−N(2)	109.6(1)
Al(1)−N(1)−Al(2)	104.17(6)	Al(2)−N(1)−C(9)	123.3(1)
Al(1)−N(1)−C(9)	114.0(1)	Al(2)−N(1)−C(10)	86.82(9)
Al(1)−N(1)−C(10)	111.2(1)		

Table 2. Selected Bond Lengths (Å) and Angles (deg) for [{^{t}BuC(N^{i}Pr)$_2$}GaMe·{^{t}BuC(N^{i}Pr)$_2$}GaMe$_2$][B(C$_6$F$_5$)$_4$] ([**7b**][B(C$_6$F$_5$)$_4$])

Ga(1)−N(1)	2.007(2)	Ga(2)−N(2)	2.037(2)
Ga(1)−N(2)	2.155(2)	Ga(2)−N(3)	1.987(2)
Ga(1)−C(1)	1.954(3)	Ga(2)−N(4)	1.973(2)
Ga(1)−C(2)	1.946(3)	Ga(2)−C(14)	1.951(3)
N(1)−C(6)	1.285(3)	N(4)−C(18)	1.338(3)
N(2)−C(6)	1.459(3)	N(3)−C(18)	1.346(3)
N(1)−Ga(1)−N(2)	64.73(9)	N(3)−Ga(2)−N(4)	67.10(9)
N(2)−Ga(1)−C(1)	116.6(1)	N(3)−Ga(2)−N(2)	114.57(9)
N(2)−Ga(1)−C(2)	117.9(1)	N(3)−Ga(2)−C(14)	122.1(1)
N(1)−Ga(1)−C(1)	113.7(1)	N(4)−Ga(2)−N(2)	114.21(9)
N(1)−Ga(1)−C(2)	111.9(1)	N(4)−Ga(2)−C(14)	119.9(1)
C(1)−Ga(1)−C(2)	119.3(1)	N(2)−Ga(2)−C(14)	112.1(1)
Ga(1)−N(2)−Ga(2)	107.08(9)	Ga(2)−N(2)−C(11)	113.9(2)
Ga(1)−N(2)−C(11)	117.3(2)	Ga(2)−N(2)−C(6)	112.5(1)
Ga(1)−N(2)−C(6)	87.4(1)	N(1)−C(6)−N(2)	108.6(2)
N(4)−C(18)−N(3)	109.2(2)		

Table 3. Selected Bond Lengths (Å) and Angles (deg) for {^{t}Bu(NCy)$_2$}Al(C$_6$F$_5$)(Me) (**11a**)

Al−N(1)	1.905(2)	Al−C(1)	1.941(3)
Al−N(2)	1.893(2)	Al−C(31)	2.011(3)
N(1)−C(2)	1.344(3)	N(2)−C(2)	1.348(3)
N(1)−Al−N(2)	69.84(9)	C(1)−Al−C(31)	116.8(2)
N(2)−Al−C(1)	120.6(1)	N(1)−Al−C(1)	119.8(1)
N(2)−Al−C(31)	109.7(1)	N(1)−Al−C(31)	111.4(1)
Al−N(1)−C(11)	137.2(2)	Al−N(2)−C(21)	133.4(2)
C(11)−N(1)−C(2)	131.7(2)	C(21)−N(2)−C(2)	132.3(2)
N(1)−C(2)−N(2)	107.8(2)		

Table 4. Selected Bond Lengths (Å) and Angles (deg) for {^{t}Bu(N^{t}Bu)$_2$}AlMe$_2$ (**12a**)

Al−N(1)	1.904(2)	Al−C(1)	1.969(2)
Al−N(2)	1.908(2)	Al−C(2)	1.967(2)
N(1)−C(3)	1.347(2)	N(2)−C(3)	1.348(2)
N(1)−Al−N(2)	68.73(7)	C(1)−Al−C(2)	115.9(1)
N(2)−Al−C(1)	116.7(1)	N(1)−Al−C(1)	117.44(9)
N(2)−Al−C(2)	115.13(9)	N(1)−Al−C(2)	114.6(1)
Al−N(1)−C(4)	127.3(1)	Al−N(2)−C(12)	128.1(1)
C(12)−N(2)−C(3)	139.4(2)	C(4)−N(1)−C(3)	139.9(2)
N(2)−C(3)−N(1)	106.0(2)		

−16.5 (br s). ^{19}F NMR (C$_6$D$_5$Cl): δ −132.5 (m, 8F, o-C$_6$F$_5$), −163.2 (t, $^3J_{FF}$ = 20, 4F, p-C$_6$F$_5$), −167.0 (br, 8F, m-C$_6$F$_5$).

Generation of [{^{t}BuC(N^{i}Pr)$_2$}Ga(Me)(NMe$_2$Ph)][B(C$_6$F$_5$)$_4$] ([8b]-[B(C$_6$F$_5$)$_4$]). [{^{t}BuC(N^{i}Pr)$_2$}GaMe$_2$·{^{t}BuC(N^{i}Pr)$_2$}GaMe][B(C$_6$F$_5$)$_4$] ([**7b**]-[B(C$_6$F$_5$)$_4$]) was generated in situ in C$_6$D$_5$Cl in a valved NMR tube as described above, and 1 equiv of NMe$_2$Ph (10.3 μL, 0.0883 mmol) was

added at 23 °C by syringe. The tube was vigorously shaken and maintained at 23 °C for 10 min. NMR spectra were then recorded and showed that complete conversion to [**8b**][B(C$_6$F$_5$)$_4$] had occurred. ^{1}H NMR (C$_6$D$_5$Cl): δ 7.21 (d, ^3J = 6.1, 2H, p-PhMe$_2$N), 7.15−7.03 (m, 8H, o- and m-PhMe$_2$N), 4.03 (septet, ^3J = 6.1, 2H, CHMe$_2$), 2.68 (s, 3H, NMe_2Ph), 1.20 (s, 9H, CMe_3), 0.67 (d, ^3J = 6.1, 6H, CHMe_2), 0.52 (d, ^3J = 5.8, CHMe_2), 0.18 (s, 3H, GaMe). ^{13}C NMR (C$_6$D$_5$Cl): δ 185.7 (s, CCMe$_3$), 149.0 (d, $^1J_{CF}$ = 241, C$_6$F$_5$), 145.2 (s, $ipso$-PhMe$_2$N), 138.8 (d, $^1J_{CF}$ = 245, C$_6$F$_5$), 136.9 (d, $^1J_{CF}$ = 243, C$_6$F$_5$), 130.4 (d, $^1J_{CH}$ = 163, p- or m-PhMe$_2$N), 120.0 (d, $^1J_{CH}$ = 161, o-PhMe$_2$N), 46.8 (d, $^1J_{CH}$ = 138, CHMe$_2$), 46.4 (q, $^1J_{CH}$ = 141, NMe_2-Ph), 28.6 (q, $^1J_{CH}$ = 129, CCMe_3), 26.7 (q, $^1J_{CH}$ = 128, CHMe_2), 26.3 (q, $^1J_{CH}$ = 129, CHMe_2), −7.1 (q, $^1J_{CH}$ = 129, GaMe). ^{11}B NMR (C$_6$D$_5$-Cl): δ −16.5 (br s). ^{19}F NMR (C$_6$D$_5$Cl): δ −132.5 (m, 8F, o-C$_6$F$_5$), −163.2 (t, $^3J_{FF}$ = 20, 4F, p-C$_6$F$_5$), −167.0 (br, 8F, m-C$_6$F$_5$).

Generation of {^{t}BuC(N^{i}Pr)$_2$}Al(Me)(C$_6$F$_5$) (9a) from 6a and B(C$_6$F$_5$)$_3$. An NMR tube was charged with {^{t}BuC(N^{i}Pr)$_2$}AlMe$_2$ (**6a**, 30.0 mg, 0.0125 mmol) and B(C$_6$F$_5$)$_3$ (63.9 mg, 0.0125 mmol), and CD$_2$Cl$_2$ (0.5 mL) was added by vacuum transfer at −78 °C. The tube was flame-sealed under vacuum, warmed to 23 °C, vigorously shaken, and maintained at 23 °C. A ^{1}H NMR spectrum was recorded immediately and showed that quantitative conversion to a 1/1 mixture of {^{t}BuC(N^{i}Pr)$_2$}Al(Me)(C$_6$F$_5$) (**9a**) and MeB(C$_6$F$_5$)$_2$ had occurred.

Data for 9a. ^{1}H NMR (CD$_2$Cl$_2$): δ 4.13 (septet, ^3J = 6.2, 2H, CHMe$_2$), 1.43 (s, CMe_3), 1.10 (d, ^3J = 6.2, 6H, CHMe_2), 0.96 (d, ^3J = 6.2, 6H, CHMe_2), −0.43 (s, 3H, AlMe). ^{13}C NMR (CD$_2$Cl$_2$):^{60} δ 181.3 (CCMe$_3$), 46.0 (CHMe$_2$), 39.6 (CCMe$_3$), 29.3 (CMe_3), 26.4 (CHMe_2), 25.5 (CHMe_2), −8.6 (br, AlMe). ^{19}F NMR (CD$_2$Cl$_2$): δ −124.1 (m, 2F, o-C$_6$F$_5$), −153.6 (m, 1F, p-C$_6$F$_5$), −162.2 (m, 2F, m-C$_6$F$_5$).

Data for MeB(C$_6$F$_5$)$_2$. ^{1}H NMR (CD$_2$Cl$_2$): δ 1.67 (s, 3H, MeB). ^{13}C NMR (C$_6$D$_5$Cl): δ 147.9 (d, $^1J_{CF}$ = 249, C$_6$F$_5$), 143.9 (d, $^1J_{CF}$ = 247, C$_6$F$_5$), 137.6 (d, $^1J_{CF}$ = 254, C$_6$F$_5$), 114.9 (br s, $ipso$-C$_6$F$_5$), 16.7 (q, $^1J_{CH}$ = 129, MeB). ^{11}B NMR (C$_6$D$_5$Cl): δ 72 (br s). ^{19}F NMR (C$_6$D$_5$-Cl): δ −129.8 (m, 4F, o-C$_6$F$_5$), −147.7 (m, 2F, p-C$_6$F$_5$), −161.7 (m, 4F, m-C$_6$F$_5$).

Generation of {^{t}BuC(N^{i}Pr)$_2$}Ga(Me)(C$_6$F$_5$) (9b) from 6b and B(C$_6$F$_5$)$_3$. An NMR tube was charged with {^{t}BuC(N^{i}Pr)$_2$}GaMe$_2$ (**6b**, 50.0 mg, 0.176 mmol) and B(C$_6$F$_5$)$_3$ (90.0 mg, 0.176 mmol), and C$_6$D$_5$-Cl (0.5 mL) was added by vacuum transfer at −78 °C. The tube was warmed to 23 °C and vigorously shaken, resulting in a colorless solution. The tube was maintained at 23 °C, and the reaction was monitored by ^{1}H NMR. The NMR spectra showed that the reaction of **6b** and B(C$_6$F$_5$)$_3$ initially yields [**7b**][MeB(C$_6$F$_5$)$_3$], which is gradually converted to {^{t}BuC(N^{i}Pr)$_2$}Ga(Me)(C$_6$F$_5$) (**9b**) and MeB(C$_6$F$_5$)$_2$. Complete conversion to **9b** and MeB(C$_6$F$_5$)$_2$ was observed after 7 h at 23 °C.

Data for 9b. ^{1}H NMR (C$_6$D$_5$Cl): δ 4.09 (septet, ^3J = 6.1 Hz, 2H, CHMe$_2$), 1.29 (s, 9H, CMe_3), 1.05 (d, ^3J = 6.5, 6H, CHMe_2), 0.95 (d, ^3J = 6.1, 6H, CHMe_2), 0.32 (s, 3H, GaMe). ^{13}C NMR (C$_6$D$_5$Cl): δ 176.9 (s, CCMe$_3$), 149.7 (d, $^1J_{CF}$ = 239, C$_6$F$_5$), 139.9 (br s, C$_6$F$_5$), 136.8 (d, $^1J_{CF}$ = 255, C$_6$F$_5$), 46.6 (d, $^1J_{CH}$ = 134, CHMe$_2$), 39.3 (s, CMe$_3$), 29.2 (q, $^1J_{CH}$ = 127, CMe_3), 26.4 (q, $^1J_{CH}$ = 119, CHMe_2), 25.5 (q, $^1J_{CH}$ = 125, CHMe_2), −4.4 (q, $^1J_{CH}$ = 123, GaMe). ^{19}F NMR (C$_6$D$_5$-Cl): δ −123.4 (m, 2F, o-C$_6$F$_5$), −155.5 (m, 1F, p-C$_6$F$_5$), −162.6 (m, 2F, m-C$_6$F$_5$).

Generation of {^{t}BuC(NCy)$_2$}Al(Me)(C$_6$F$_5$) (11a) from 10a and B(C$_6$F$_5$)$_3$. An NMR tube was charged with {^{t}BuC(NCy)$_2$}AlMe$_2$ (**10a**, 21.0 mg, 0.0125 mmol) and B(C$_6$F$_5$)$_3$ (63.9 mg, 0.0125 mmol), and CD$_2$Cl$_2$ was added by vacuum transfer. The tube was flame-sealed under vacuum, warmed to 23 °C, and vigorously shaken. A ^{1}H NMR spectrum was recorded immediately and showed that quantitative formation of a 1/1 mixture of {^{t}BuC(NCy)$_2$}Al(Me)(C$_6$F$_5$) (**11a**) and MeB(C$_6$F$_5$)$_2$ had occurred.

Data for 11a. ^{1}H NMR (CD$_2$Cl$_2$): δ 3.21 (br, 2H, NCH), 1.85−1.65 (br, 8H, Cy), 1.50−1.05 (br, 12H, Cy), 1.30 (s, 9H, CMe_3), −0.78 (br s, 3H, AlMe). ^{19}F NMR (CD$_2$Cl$_2$): δ −123.5 (m, 2F, o-C$_6$F$_5$), −152.5 (m, 1F, p-C$_6$F$_5$), −162.9 (m, 2F, m-C$_6$F$_5$).

{^{t}BuC(N^{t}Bu)$_2$}AlMe$_2$ (12a). A colorless solution of ^{t}BuC=N=C^t-Bu (2.00 g, 13.0 mmol) in Et$_2$O (35 mL) was cooled to 0 °C, and

---

(60) The AlC$_6$F$_5$ and MeB(C$_6$F$_5$)$_2$ resonances are significantly overlapped and therefore are not listed here.

Table 5. Summary of Crystal Data for Compounds [**4a**][B(C₆F₅)₄], [**7b**][B(C₆F₅)₄], **11a**, and **12a**

	complex			
	[**4a**][B(C₆F₅)₄]	[**7b**][B(C₆F₅)₄]	**11a**	**12a**
formula	C₅₅H₅₉Al₂BF₂₀N₄	C₄₉H₅₅BF₂₀Ga₂N₄	C₂₄H₃₄AlF₅N₂	C₁₅H₃₃AlN₂
fw	1220.83	1230.22	472.51	268.41
crystal size (mm)	0.45 × 0.40 × 0.34	0.46 × 0.43 × 0.42	0.56 × 0.18 × 0.17	0.43 × 0.42 × 0.37
d (calc), Mg/m³	1.448	1.536	1.266	1.006
crystal system	triclinic	triclinic	monoclinic	trigonal
space group	$P\bar{1}$	$P\bar{1}$	$P2_1/n$	$P3_221$
a, Å	12.2334(8)	14.0186(7)	13.161(2)	9.3599(4)
b, Å	12.4767(8)	18.8356(9)	15.336(2)	9.3599(4)
c, Å	18.800(1)	21.689(1)	12.441(2)	35.044(2)
α, deg	92.832(1)	101.326(1)		
β, deg	102.235(1)	90.239(1)	99.29(2)	
γ, deg	90.305(1)	108.236(1)		
V, Å³	2800.6(3)	5320.1(4)	2478.1(6)	2658.8(2)
Z	2	4	4	6
T (K)	173(2)	173(2)	200(2)	173(2)
diffractometer	Bruker CCD-1000	Bruker CCD-1000	Enraf-Nonius CAD4	Bruker CCD-1000
radiation, λ (Å)	Mo Kα, 0.710 73	Mo Kα, 0.710 73	Mo Kα, 0.710 10	Mo Kα, 0.710 73
2θ range (deg)	4.68 < 2θ < 52.74	3.32 < 2θ < 52.74	4.0 < 2θ < 50.0	5.02 < 2θ < 56.58
index ranges: h; k; l	−15,14; ±15; 0,23	±17; ±23; 0,27	−15,2; −18,1; ±14	−12,11; −12,9; −46,12
no. of reflns	19 923	47 676	5189	12 044
no. of unique reflns	11 240	21 513	4240	4083
R_{int}	0.019	0.025	0.021	0.020
μ, mm⁻¹	0.160	1.121	0.133	0.104
transmission coefficients (%)		0.650/0.627		0.962/0.957
structure solution	direct methods[a]	direct methods[a]	direct methods[b,c]	direct methods[a]
data/restraints/parameters	11 240/0/744	21 513/0/1403	4240/0/425	4083/30/236
GOF on F^2	1.011	1.021	1.109	1.061
R indices ($I > 2\sigma(I)$)[d,e]	R1 = 0.0360	R1 = 0.0388	R1 = 0.0408	R1 = 0.0494
	wR2 = 0.0796	wR2 = 0.0927	wR2 = 0.0829	wR2 = 0.1312
R indices (all data)[d,e]	R1 = 0.0635	R1 = 0.0619	R1 = 0.0926	R1 = 0.0571
	wR2 = 0.0868	wR2 = 0.1017	wR2 = 0.1063	wR2 = 0.1357
max resid density (e/Å³)	0.268	2.164	0.221	0.337

[a] SHELXTL-Version 5.1, Bruker Analytical X-ray Systems, Madison, WI. [b] SHELXTL-Plus Version 5, Siemens Industrial Automation, Inc., Madison, WI. [c] MULTAN, Multan80., University of York, York, England. [d] $R1 = \Sigma||F_o| - |F_c||/\Sigma|F_o|$ [e] $wR2 = [\Sigma[w(F_o^2 - F_c^2)^2]/\Sigma[w(F_o^2)^2]]^{1/2}$, where $w = q/\sigma^2(F_o^2) + (aP)^2 + bP$.

*t*BuLi (7.62 mL of 1.7 M solution in pentane, 13.0 mmol) was added dropwise by syringe. The mixture was allowed to warm to room temperature and was stirred for 1 h, resulting in a white slurry. The mixture was cooled to 0 °C, and a colorless solution of AlClMe₂ (1.20 g, 13.0 mmol) in Et₂O (10 mL), which was also cooled to 0 °C, was added dropwise. The resulting mixture was allowed to warm to room temperature and was stirred for 12 h, affording a slurry of a white solid in a pale yellow solution. The mixture was filtered. The volatiles were removed from the filtrate under vacuum to afford a colorless solid as a crude product. Sublimation of the crude product (70 °C, <0.001 mmHg) to a −78 °C coldfinger afforded {*t*BuC(N*t*Bu)₂}AlMe₂ (1.3 g, 37%) as colorless block crystals. ¹H NMR (C₆D₆): δ 1.34 (s, 18H, NC*Me₃*), 1.20 (s, 9H, CC*Me₃*), −0.21 (s, 6H, Al*Me₂*). ¹³C NMR (C₆D₆): δ 181.9 (N*C*N), 53.4 (N*C*Me₃), 37.5 (C*C*Me₃), 34.0 (NC*Me₃*), 31.6 (CC*Me₃*), −7.1 (Al*Me₂*). EI-MS (*m/z*): 57 (AlMe₂⁺, 46). Anal. Calcd for C₁₅H₃₃AlN₂: C, 67.10; H, 12.41; N, 10.44. Found: C, 67.43; H, 12.54; N, 10.70.

Generation of [{*t*BuC(N*t*Bu)₂}AlMe][B(C₆F₅)₄] ([13a][B(C₆F₅)₄]). An NMR tube was charged with {*t*BuC(N*t*Bu)₂}AlMe₂ (**12a**, 17 mg, 0.064 mmol) and [Ph₃C][B(C₆F₅)₄] (58 mg, 0.064 mmol), and C₆D₅Cl (0.5 mL) was added by vacuum transfer at −78 °C. The tube was flame-sealed under vacuum, warmed to 23 °C, and vigorously shaken. A dark brown solution formed. The tube was maintained at 23 °C for 5 min. A ¹H NMR spectrum was recorded and showed that quantitative conversion to a 1/1 mixture of [**13a**][B(C₆F₅)₄] and Ph₃CCH₃ had occurred. ¹H NMR (C₆D₅Cl): δ 1.22 (s, 9H, CC*Me₃*), 1.20 (s, 18H, NC*Me₃*), −0.04 (s, 3H, Al*Me*). ¹³C NMR (C₆D₅Cl): δ 189.5 (*C*CMe₃), 149.0 (d, ¹*J*_CF = 241, *C₆F₅*), 138.8 (d, ¹*J*_CF = 245, *C₆F₅*), 136.9 (d, ¹*J*_CF = 243, *C₆F₅*), 54.5 (NC*Me₃*), 36.1 (CC*Me₃*), 34.3 (NC*Me₃*), 32.0 (CC*Me₃*), −2.9 (Al*Me*). ¹¹B NMR (C₆D₅Cl): δ −16.5 (br s). ¹⁹F NMR (C₆D₅Cl): δ −132.5 (m, 8F, *C₆F₅*), −163.2 (t, ³*J*_FF = 20, 4F, *C₆F₅*), −167.0 (br, 8F, *C₆F₅*).

Generation of [{*t*BuC(N*t*Bu)₂}GaMe][B(C₆F₅)₄] ([13b][B(C₆F₅)₄]).

An NMR tube was charged with {*t*BuC(N*t*Bu)₂}GaMe₂ (**12b**, 20 mg, 0.064 mmol) and [Ph₃C][B(C₆F₅)₄] (58 mg, 0.064 mmol), and C₆D₅Cl (0.5 mL) was added by vacuum transfer at −78 °C. The tube was flame-sealed under vacuum, warmed to 23 °C, and vigorously shaken. A dark brown solution formed. The tube was maintained at 23 °C for 30 min. A ¹H NMR spectrum was recorded and showed that quantitative conversion to a 1/1 mixture of [**13b**][B(C₆F₅)₄] and Ph₃CCH₃ had occurred. ¹H NMR (C₆D₅Cl): δ 1.15 (s, 9H, CC*Me₃*), 1.11 (s, 18H, NC*Me₃*), 0.35 (s, 3H, Ga*Me*). ¹³C NMR (C₆D₅Cl): δ 191.4 (*C*CMe₃), 149.0 (d, ¹*J*_CF = 241, *C₆F₅*), 138.8 (d, ¹*J*_CF = 245, *C₆F₅*), 136.9 (d, ¹*J*_CF = 243, *C₆F₅*), 56.4 (NC*Me₃*), 38.1 (CC*Me₃*), 33.6 (NC*Me₃*), 30.4 (CC*Me₃*), 0.2 (Ga*Me*). ¹¹B NMR (C₆D₅Cl): δ −16.5 (br s). ¹⁹F NMR (C₆D₅Cl): δ −132.5 (m, 8F, *C₆F₅*), −163.2 (t, ³*J*_FF = 20, 4F, *C₆F₅*), −167.0 (br, 8F, *C₆F₅*).

Generation of [{*t*BuC(N*t*Bu)₂}Ga(Me)(NMe₂Ph)][B(C₆F₅)₄] ([14b]-[B(C₆F₅)₄]). A solution of [{*t*BuC(N*t*Bu)₂}GaMe][B(C₆F₅)₄] ([**13b**]-[B(C₆F₅)₄]) in C₆D₅Cl (0.5 mL) was generated in an NMR tube as described above. The tube was maintained at 23 °C for 30 min, and 1 equiv of NMe₂Ph (4.1 μL, 0.064 mmol) was added at 23 °C by syringe. The tube was maintained at 23 °C for 10 min. NMR spectra were recorded and showed that quantitative conversion to [**14b**][B(C₆F₅)₄] had occurred. ¹H NMR (C₆D₅Cl): δ 7.18 (t, ³*J* = 7.2, 4H, *m-Ph*), 6.90 (t, ³*J* = 7.6, 2H, *p-Ph*), 6.77 (d, ³*J* = 8.6, 4H, *o-Ph*), 2.66 (s, 3H, N*Me*), 1.32 (s, 18H, NC*Me₃*), 1.16 (s, 9H, CC*Me₃*), 0.12 (s, 3H, Ga*Me*). ¹³C NMR (C₆D₅Cl): δ 190.5 (*C*CMe₃), 149.0 (d, ¹*J*_CF = 241, *C₆F₅*), 145.5 (*ipso-Ph*), 138.8 (d, ¹*J*_CF = 245, *C₆F₅*), 136.9 (d, ¹*J*_CF = 243, *C₆F₅*), 129.4 (*p-* or *m-Ph*), 128.4 (*p-* or *m-Ph*), 119.9 (*o-Ph*), 55.9 (NC*Me₃*), 46.4 (N*Me*), 36.5 (CC*Me₃*), 34.0 (NC*Me₃*), 31.1 (CC*Me₃*), −3.4 (Ga*Me*). ¹¹B NMR (C₆D₅Cl): δ −16.5 (br s). ¹⁹F NMR (C₆D₅Cl): δ −132.5 (m, 8F, *o-C₆F₅*), −163.2 (t, ³*J*_FF = 20, 4F, *o-C₆F₅*), −167.0 (br s, 8F, *m-C₆F₅*).

NMR Simulations. NMR spectra were simulated using the software package gNMR (version 3.6 for Macintosh, Cherwell Scientific

Publishing Limited), in which the evaluation of static spectra is based on general NMR theory[61] and the evaluation of dynamic spectra involving chemical exchange is based on the standard Louiville representation of quantum mechanics, as described by Binsch.[62,63] A Lorentzian line shape was assumed for all the calculated spectra.

X-ray Crystallography. The structure of [**2a**][B(C_6F_5)$_4$] was determined by V. G. Young, Jr. (University of Minnesota). The structure of **11a** was determined by D. C. Swenson (University of Iowa), and the structures of [**4a**][B(C_6F_5)$_4$], [**7b**][B(C_6F_5)$_4$], and **12a** were determined by I. A. Guzei (Iowa State University). Crystal data, data collection details, metrical parameters, and solution refinement procedures are collected in Tables 1−5, except those for [**2a**][B(C_6F_5)$_4$], which are listed in the Supporting Information.

[{MeC(N^{i}Pr)$_2$}$_2$Al$_2$Me$_3$][B(C_6F_5)$_4$] ([2a][B(C_6F_5)$_4$]): crystals were grown by crystallization from a 10/1 mixture of hexane and toluene (5 mL). Pure [**2a**][B(C_6F_5)$_4$] (100 mg) was dissolved in toluene (0.5 mL) in a sample tube, and hexane (5 mL) was added very slowly to form a top layer. The two layers were allowed to diffuse at 23 °C for 5 d to afford small crystals of poor quality which formed at the interface of the two layers. Crystallographic details are given in the Supporting Information. The dearth of observed data precluded a fully anisotropic refinement. Only the Al atoms were refined anisotropically. The cell constants and metrical parameters should be considered approximate because of the presence of a satellite crystal; however, the atom connectivity is established to be analogous to that of [**2a**][B(C_6F_5)$_4$].

[{MeC(NCy)$_2$}$_2$Al$_2$Me$_3$][B(C_6F_5)$_4$] ([4a][B(C_6F_5)$_4$]): crystals were grown by crystallization from a mixed solvent system of 10/10/1/1 hexane/pentane/C_6D_5Cl/ClCD$_2$CD$_2$Cl. Pure [**4a**][B(C_6F_5)$_4$] (100 mg) was dissolved in a 1/1 mixture of C_6D_5Cl and ClCD$_2$CD$_2$Cl (0.2 mL), and a 1/1 mixture of hexane and pentane (2 mL) was added very slowly to form a top layer. The two layers were allowed to diffuse at 23 °C for 3 d to afford large crystals which formed at the interface of the two layers. All non-H atoms were refined anisotropically, and all H-atoms were placed in ideal positions and refined as riding atoms with relative isotropic displacement coefficients.

[{^{t}BuC(N^{i}Pr)$_2$}GaMe·{^{t}BuC(N^{i}Pr$_2$}GaMe$_2$][B(C_6F_5)$_4$] ([7b][B(C_6F_5)$_4$]): crystals were grown from a 10/10/1 hexane/pentane/C_6D_5Cl mixed solvent system. The salt was dissolved in C_6D_5Cl (0.1 mL), and a 1/1 mixture of hexane/pentane (2 mL) was slowly added to form a top layer. The two layers were allowed to diffuse at 23 °C for 2 d to afford large crystals which formed at the interface of the two layers. All non-H atoms were refined anisotropically, and all H-atoms were placed in ideal positions and refined as riding atoms with relative isotropic displacement coefficients. There are two independent molecules of [**7b**][B(C_6F_5)$_4$] in the asymmetric unit. The two **7b**$^+$ cations differ in the rotational conformation around the Ga−N$_{(\mu-\text{amidinate})}$ bond but exhibit very similar bond lengths and angles, while the two B(C_6F_5)$_4$$^-$ anions are identical.

{^{t}BuC(NCy)$_2$}Al(Me)(C_6F_5) (11a): crystals were grown from a saturated pentane solution at −78 °C. All non-H atoms were refined anisotropically, and all H-atoms were refined isotropically.

{^{t}BuC(N^{t}Bu)$_2$}AlMe$_2$ (12a): crystals were grown by slow sublimation of crude **12a** (70 °C, <0.001 mmHg, 1 d). Pure **12a** was collected as colorless crystals on a −78 °C cold probe. All non-H atoms were refined anisotropically, and all H-atoms were placed in ideal positions and refined as riding atoms with relative isotropic displacement coefficients. There is positional disorder in the structure: atoms C(5), C(6), and C(7) are equally disordered over two positions each in a 65/35 ratio. The distances between the tertiary carbon atoms and the disordered methyl carbons were restrained to be identical within 0.002 Å.

Supporting Information Available: Tables of atomic coordinates, isotropic displacement parameters, anisotropic displacement parameters, and bond distances and bond angles for [**2a**][B(C_6F_5)$_4$], [**4a**][B(C_6F_5)$_4$], [**7b**][B(C_6F_5)$_4$], **11a**, and **12a**, and details concerning crystal data, data collection, and solution and refinement for [**2a**][B(C_6F_5)$_4$] (PDF). This material is available free of charge via the Internet at http://pubs.acs.org.

JA992104J

(61) Pople, J. A.; Schneider, W. G.; Bernstein, H. J. *High-Resolution Nuclear Magnetic Resonance*; McGraw-Hill: New York, NY, 1959.

(62) (a) Binsch, G. In *Dynamic Nuclear Magnetic Resonance Spectroscopy*; Jackman, L. M., and Cotton, F. A., Eds.; Academic Press: London, 1975; p 45. (b) Steigel, A. In *NMR, Basic Principles and Progress*; Diehl, P., Fluck, E., Kosfeld, R., Eds.; Springer-Verlag: Berlin, 1978; Vol. 15, p 1.

(63) (a) Binsch, G. *J. Am. Chem. Soc.* **1969**, *91*, 1304. (b) Stephenson, D. S.; Binsch, G. *J. Magn. Reson.* **1978**, *30*, 625.